The coupling of homogeneous models for two-phase flows

Annalisa Ambroso, Christophe Chalons, Frédéric Coquel, Edwige Godlewski, Frédéric Lagoutière, Pierre-Arnaud Raviart, Nicolas Seguin

The coupling of homogeneous models for two-phase flows

Annalisa Ambroso[1], Christophe Chalons[2], Frédéric Coquel[3], Edwige Godlewski[3], Frédéric Lagoutière[2], Pierre-Arnaud Raviart[3], Nicolas Seguin[3]

[1] *DEN/DM2S/SFME/LETR CEA-Saclay, F-91191 Gif-sur-Yvette, France,*
[2] *Université Paris 7-Denis Diderot et UMR 7598 Laboratoire Jacques-Louis Lions, Paris, F-75005 France,*
[3] *Université Pierre et Marie Curie-Paris6, UMR 7598 LJLL, Paris, F-75005 France; CNRS, UMR 7598 LJLL, Paris, F-75005 France*

annalisa.ambroso@cea.fr, chalons@math.jussieu.fr, coquel@ann.jussieu.fr, godlwski@ann.jussieu.fr, lagoutie@math.jussieu.fr, raviart@ann.jussieu.fr, seguin@ann.jussieu.fr

Abstract

We consider the numerical coupling at a fixed spatial interface of two homogeneous models used for describing non isothermal compressible two phase flows. More precisely, we concentrate on the numerical coupling of the homogeneous equilibrium model and the homogeneous relaxation model in the context of finite volume methods. Three methods of coupling are presented. They are based on one of the following requirements: continuity of the conservative variable through the coupling interface, continuity of the primitive variable and global conservation of mass, momentum and energy. At the end, several numerical experiments are presented in order to illustrate the ability of each method to provide results in agreement with their principle of construction.

1 Introduction

The coupling of fluid flow models is becoming a key topic in industrial code development. From an engineering point of view, different models are used to treat different sub-domains of a complex system where a flow takes place. Therefore it is natural to want to have a global simulation for the system by putting these domains, and thus these models, side to side. This rises the delicate question of the continuity of the description of the flow. As an example, think of the simulation of a combustion engine, where the *natural* models for the fuel pipes, the injector and the combustion chamber are clearly different, or, again, think of the treatment, in nuclear energy industry, of the coolant circuits which are formed by different components, each one with its associated specific model for the coolant flow. Our work is motivated by this last application and the coolant under consideration is a two-phase fluid.

Two-phase flows can be described by means of different models: mixture, drift (homogeneous or not), two-fluid or even multi-field models are currently used in industrial thermo-hydraulic codes. We consider here the problem of the interfacial coupling of two models, *i.e.* we imagine that a two-phase flow is described by means of a model M_1 at the left of a fictitious interface $\mathcal{I}$ and by another model M_2 at the right of $\mathcal{I}$. Our aim is to numerically describe the whole flow dealing with the potential discontinuities at $\mathcal{I}$, when the model jumps. It is clear that this analysis strongly depends on the two models M_1 and M_2 that describe the flow on each side of the discontinuity.

In this paper we focus on the coupling of two homogeneous models. More precisely, we consider as M_1 a homogeneous equilibrium model frequently referred to as HEM and, as model M_2 a homogeneous relaxation model HRM. Homogeneous models describe a two-component flow as the flow of a single fluid: the compound. A description of these models can be found in [10], [22]. When the two components are assumed to follow a perfect gas law, the full thermodynamic of the compound can be described by means of analytic formulas, as it is clearly presented in [30] and in [13], [15], [16], [17]. We will focus on this case and, for the sake of completeness, we present these models in Section 2. The HEM model is detailed in Section 2.2.1 while Section 2.2.2 details the HRM one.

The general framework of the coupling problem is as follows. Let $\mathcal{D}$ be an open subset of $\mathbb{R}^n$ ($n \in \mathbb{N}, n \geq 1$) divided in two separated open sub-domains $\mathcal{D}^{\mathrm{E}}$ and $\mathcal{D}^{\mathrm{R}}$ and an interface $\mathcal{I}$: $\mathcal{D} = \mathcal{D}^{\mathrm{E}} \cup \mathcal{D}^{\mathrm{R}} \cup \mathcal{I}$. We assume that the flow evolves according to HEM in $\mathcal{D}^{\mathrm{E}}$ and HRM in $\mathcal{D}^{\mathrm{R}}$. We note $\mathbf{u}^{\mathrm{E}}$ and $\mathbf{u}^{\mathrm{R}}$ the vectors of the corresponding conservative unknowns. In the following, we restrict the study to the one-dimensional case where $\mathcal{D}^{\mathrm{E}} = \mathbb{R}^-$, $\mathcal{D}^{\mathrm{R}} = \mathbb{R}^+$ and $\mathcal{I} = \{0\}$. Therefore, the flow is described by the following problem

$$\begin{array}{c|c} \text{HEM on } \mathbb{R}^+ \times \mathcal{D}^{\mathrm{E}} & \text{HRM on } \mathbb{R}^+ \times \mathcal{D}^{\mathrm{R}} \\ \partial_t \mathbf{u}^{\mathrm{E}} + \partial_x \mathbf{f}^{\mathrm{E}}(\mathbf{u}^{\mathrm{E}}) = \mathbf{S}^{\mathrm{E}}(\mathbf{u}^{\mathrm{E}}), & \partial_t \mathbf{u}^{\mathrm{R}} + \partial_x \mathbf{f}^{\mathrm{R}}(\mathbf{u}^{\mathrm{R}}) = \mathbf{S}^{\mathrm{R}}(\mathbf{u}^{\mathrm{R}}), \end{array} \tag{1}$$

where $\mathbf{f}^{\mathrm{E}}, \mathbf{f}^{\mathrm{R}}$ and $\mathbf{S}^{\mathrm{E}}, \mathbf{S}^{\mathrm{R}}$ respectively denote the conservative flux and the source terms of the models, that will be given in Section 2. We underline the lack of information at the interface $\mathcal{I}$. Our only constraint is given by the context of the problem. We know that the physical entity we are describing is the same: the flow of the same fluid. Its properties are characterized by $\mathbf{u}^E$ on one side of the interface and by $\mathbf{u}^R$ on the other side, and we wish to link these quantities at the crossing of $\mathcal{I}$ taking into account the continuity of the flow.

We acknowledge the artificial character of this problem: the real physics is the same, but, when different codes are used to simulate it, the global description can be discontinuous. This can be seen as an artificial error introduced by the simulation process. Our analysis wants to deal with this error and its effects on the solution of the problem.

First of all, the problem must be analyzed from the modelling point of view. To make (1) complete, we need to add an *interface model*, that is to say, we must detail the properties of the flow that should hold at the crossing of the interface. We think, for instance, of the continuity of some variables or the conservation of some quantities. In a second place, the global problem should be analyzed mathematically. Compatibility of the constraints imposed at the interface within one another and with the models should be checked. Moreover, we point out that, due to the hyperbolic character of the models under consideration (see Section 2), it is very likely that a given coupling problem with a prescribed model for the interface cannot be solved for all initial data. Finally, we must not forget that we are interested in the *numerical* simulation of the flow. This has two main implications. On the one hand, we wish that the constraints given by the chosen *interface model* lead to simple numerical relations. On the other hand, we must keep in mind that the strategy of coupling we choose can be effective only if its numerical treatment is appropriate.

The problem of coupling nonlinear conservation laws was first addressed in [25] and in [26]. In [4] and in [5] a study of the case where the models to be coupled are given by two Euler systems for gas dynamics with two different equations of state is presented. In this case, one of the numerical techniques proposed is very similar to the *ghost fluid* method ([32], [2]). The coupling between a one-dimensional model of gas dynamics and a 2-dimensional one are treated in [28]. References [27] and [11] study the case of a change of porosity of the medium where the flow takes place, while [33] and [35] deal with the coupling of acoustic wave equations with different sound speed. For the case under study in the present article, *i.e.* the coupling of a Homogeneous Relaxation Model with a Homogeneous Equilibrium Model, some results were presented in [6] and a study of an industrial case of interest can be found in [29].

In this paper, we propose several ways for numerically solving the coupling problem (1), depending on the treatment we impose at the interface $\mathcal{I}$. The HRM and HEM models are presented in Section 2. The *interface models* we consider are listed in Section 3. In Section 4 we give the basis for the numerical treatment of the problem. In particular, we present the two main strategies that can be chosen: the flux coupling (Section 4.1.1) and the intermediate state coupling (Section 4.1.2). Section 4 ends with a description of the numerical schemes we consider.
Numerical tests to illustrate the different choices are presented in Section 5, followed by a conclusion (Section 6).

2 Governing equations and physical modelling

In this study, we focus on the one-dimensional case ($n = 1$) and we set $\mathcal{D} = \mathbb{R}$, $\mathcal{D}^{\mathrm{E}} = \mathbb{R}^{-,*}$ and $\mathcal{D}^{\mathrm{R}} = \mathbb{R}^{+,*}$. The coupling interface is then located at $x = 0$: $\mathcal{I} = \{x = 0\}$. Let us now precise the general modelling assumptions on the two-phase flow.

2.1 General modelling assumptions

We follow [13], [15], [16], [17], [30] and consider that each phase is a fluid with its own thermodynamic properties. Let us begin by introducing some notations for the two phases. In the following, ρ_α, ε_α, $p_\alpha(\rho_\alpha, \varepsilon_\alpha)$ and $T_\alpha(\rho_\alpha, \varepsilon_\alpha)$ respectively denote the density, the internal energy, the pressure and the temperature of the phase $\alpha = 1, 2$. Then, the entropy $\eta_\alpha(\rho_\alpha, \varepsilon_\alpha)$ is defined up to an additive constant via Gibbs relations, that is

$$\frac{\partial \eta_\alpha}{\partial \varepsilon_\alpha}(\rho_\alpha, \varepsilon_\alpha) = \frac{1}{T_\alpha(\rho_\alpha, \varepsilon_\alpha)}, \quad \frac{\partial \eta_\alpha}{\partial \rho_\alpha}(\rho_\alpha, \varepsilon_\alpha) = -\frac{p_\alpha(\rho_\alpha, \varepsilon_\alpha)}{\rho_\alpha^2 T_\alpha(\rho_\alpha, \varepsilon_\alpha)}. \tag{2}$$

In order to make the localization of phase changes possible, we introduce an order parameter $z \in [0, 1]$ that equals 1 in phase 1 and 0 in phase 2.

The matter is now to put these two fluids in relation in a way to obtain a thermodynamically coherent description of the two-phase flow. With this in mind, we adopt the following definitions for the mixture density ρ, internal energy ε and pressure p:

$$\begin{cases} \rho = z\rho_1 + (1-z)\rho_2, \\ \rho\varepsilon = z\rho_1\varepsilon_1 + (1-z)\rho_2\varepsilon_2, \\ p = zp_1(\rho_1, \varepsilon_1) + (1-z)p_2(\rho_2, \varepsilon_2). \end{cases} \tag{3}$$

Then, we make the assumption that the two fluids have the same temperature. Therefore, we impose the following closure relation which defines the mixture temperature T

$$T = T_1(\rho_1, \varepsilon_1) = T_2(\rho_2, \varepsilon_2). \tag{4}$$

We complete this section by giving explicit formulas for p_α and T_α, $\alpha = 1, 2$. We consider the case of perfect gas equations of state given by

$$\begin{cases} p_\alpha(\rho_\alpha, \varepsilon_\alpha) = (\gamma_\alpha - 1)\rho_\alpha\varepsilon_\alpha, \\ T_\alpha(\rho_\alpha, \varepsilon_\alpha) = \dfrac{\varepsilon_\alpha}{C_{v,\alpha}}, \end{cases} \qquad \alpha = 1, 2, \tag{5}$$

with different adiabatic coefficients $\gamma_1 > 1$ and $\gamma_2 > 1$. We choose $\gamma_2 < \gamma_1$ without loss of generality. For simplicity reasons, specific heats $C_{v,1}$ and $C_{v,2}$ are assumed to be equal and we set

$$C_v = C_{v,1} = C_{v,2} > 0. \tag{6}$$

This hypothesis is widely used in the litterature ([13], [15], [16], [17], [30]) and allows to ease the computations. For the general case with different specific heat coefficients for the two fluids, we refer to [23] and [3].
As an immediate consequence of (3)-(4)-(6), we thus have

$$\varepsilon = \varepsilon_1 = \varepsilon_2 = C_v T. \tag{7}$$

Integrating Gibbs relations (2), we then define entropies η_α by

$$\eta_\alpha(\rho_\alpha, \varepsilon_\alpha) = C_{v,\alpha} \ln \frac{p_\alpha(\rho_\alpha, \varepsilon_\alpha)}{\rho_\alpha^{\gamma_\alpha}}, \quad \alpha = 1, 2. \tag{8}$$

2.2 Governing equations

In this section, we describe the basic assumptions that lead to the homogeneous equilibrium model HEM and to the homogeneous relaxation model HRM and we give the two sets of equations associated with them. We begin by HEM.

2.2.1 The homogeneous equilibrium model HEM

The homogeneous equilibrium model is obtained under specific assumptions of mechanical and thermodynamic equilibrium for the two phase flow. This means that when both phases are present, their pressures $p_\alpha(\rho_\alpha, \varepsilon_\alpha)$ and their free enthalpies $g_\alpha(\rho_\alpha, \varepsilon_\alpha) = \varepsilon_\alpha + p_\alpha(\rho_\alpha, \varepsilon_\alpha)/\rho_\alpha - \eta_\alpha(\rho_\alpha, \varepsilon_\alpha)T_\alpha(\rho_\alpha, \varepsilon_\alpha)$ are equal:

$$\left\{ \begin{array}{l} p_1(\rho_1, \varepsilon_1) = p_2(\rho_2, \varepsilon_2), \\ g_1(\rho_1, \varepsilon_1) = g_2(\rho_2, \varepsilon_2), \end{array} \right. \tag{9}$$

For the perfect gas mixture described above, this is equivalent to

$$\left\{ \begin{array}{l} (\gamma_1 - 1)\rho_1 = (\gamma_2 - 1)\rho_2, \\ (\gamma_1 - 1) - \ln \dfrac{(\gamma_1 - 1)}{\rho_1^{(\gamma_1 - 1)}} = (\gamma_2 - 1) - \ln \dfrac{(\gamma_2 - 1)}{\rho_2^{(\gamma_2 - 1)}}, \end{array} \right. \tag{10}$$

thanks to (5)-(7)-(8). By easy calculations, we get

Proposition 2.1 *System (10) admits a unique solution $(\rho_1^\star, \rho_2^\star)$ given by*

$$\left\{ \begin{array}{l} \rho_1^\star = \dfrac{1}{e}\left(\dfrac{\gamma_2 - 1}{\gamma_1 - 1}\right)^{\dfrac{\gamma_2}{\gamma_2 - \gamma_1}}, \\ \rho_2^\star = \dfrac{1}{e}\left(\dfrac{\gamma_2 - 1}{\gamma_1 - 1}\right)^{\dfrac{\gamma_1}{\gamma_2 - \gamma_1}}. \end{array} \right. \tag{11}$$

Remark 1 Under assumption $\gamma_2 < \gamma_1$, we have $\rho_1^\star < \rho_2^\star$.

At this stage, it is important to notice that considering perfect gas equations of state with the same specific heats leads to explicit and simple formulas for equilibrium densities $\rho_1^\star$ and $\rho_2^\star$. This is actually the main motivation for such a choice. As an immediate consequence of (6), note also that $\rho_1^\star$ and $\rho_2^\star$ do not depend on the mixture temperature T.

Remark 2 Entropies η_α being defined up to an additive constant, one could have set

$$\eta_\alpha(\rho_\alpha, \varepsilon_\alpha) = C_{v,\alpha} \ln \frac{p_\alpha(\rho_\alpha, \varepsilon_\alpha)}{\rho_\alpha^{\gamma_\alpha}} - \gamma_\alpha C_{v,\alpha} \ln(\gamma_\alpha - 1)C_{v,\alpha}, \quad \alpha = 1, 2, \tag{12}$$

instead of (8). In this case, $\rho_1^\star$ and $\rho_2^\star$ are given by

$$\left\{ \begin{array}{l} \rho_1^\star = \exp\left(-1 - \dfrac{\gamma_2 \ln(\gamma_2 - 1)C_v - \gamma_1 \ln(\gamma_1 - 1)C_v}{\gamma_2 - \gamma_1}\right) \times \left(\dfrac{\gamma_2 - 1}{\gamma_1 - 1}\right)^{\dfrac{\gamma_2}{\gamma_2 - \gamma_1}}, \\ \rho_2^\star = \exp\left(-1 - \dfrac{\gamma_2 \ln(\gamma_2 - 1)C_v - \gamma_1 \ln(\gamma_1 - 1)C_v}{\gamma_2 - \gamma_1}\right) \times \left(\dfrac{\gamma_2 - 1}{\gamma_1 - 1}\right)^{\dfrac{\gamma_1}{\gamma_2 - \gamma_1}}, \end{array} \right. \tag{13}$$

or, in an equivalent way,

$$\left\{\begin{array}{l} \rho_1^\star = \exp\left(\dfrac{\gamma_1 + (\gamma_1-1)\ln(\gamma_1-1)C_v - \gamma_2 - (\gamma_2-1)\ln(\gamma_2-1)C_v}{\gamma_2-\gamma_1}\right) \\ \qquad\qquad \times \left(\dfrac{\gamma_2-1}{\gamma_1-1}\right)^{\dfrac{\gamma_2-1}{\gamma_2-\gamma_1}}, \\ \rho_2^\star = \exp\left(\dfrac{\gamma_1 + (\gamma_1-1)\ln(\gamma_1-1)C_v - \gamma_2 - (\gamma_2-1)\ln(\gamma_2-1)C_v}{\gamma_2-\gamma_1}\right) \\ \qquad\qquad \times \left(\dfrac{\gamma_2-1}{\gamma_1-1}\right)^{\dfrac{\gamma_1-1}{\gamma_2-\gamma_1}}, \end{array}\right. \tag{14}$$

which corresponds to the values proposed in [13].

This result implies that in the HEM framework, the densities ρ_α of each phase are given fixed values when both phases are present, *i.e.* when order parameter $z \in (0,1)$. The mixture density $\rho = \rho_1^\star z + \rho_2^\star(1-z)$ thus lies in the interval $[\rho_1^\star, \rho_2^\star]$ and depends on the value of z. Concerning the pressure law p, we have $p(\rho,\varepsilon) = p_1(\rho_1^\star,\varepsilon_1) = p_2(\rho_2^\star,\varepsilon_2)$ for all $\rho \in [\rho_1^\star,\rho_2^\star]$ which corresponds to the first assumption in (9). Outside this interval, it can be naturally extended since only phase 1 (respectively phase 2) is present when $0 < \rho \leq \rho_1^\star$ (respectively $\rho \geq \rho_2^\star$). We get

$$p(\rho,\varepsilon) = \left\{\begin{array}{ll} (\gamma_1-1)\rho\varepsilon & \text{if} \quad \rho \leq \rho_1^\star, \\ (\gamma_1-1)\rho_1^\star\varepsilon = (\gamma_2-1)C_v\rho_2^\star T & \text{if} \quad \rho_1^\star < \rho < \rho_2^\star, \\ (\gamma_2-1)\rho\varepsilon & \text{if} \quad \rho \geq \rho_2^\star. \end{array}\right. \tag{15}$$

In the following, this pressure law will be noted $p^{\mathrm{E}}(\rho,\varepsilon)$.

Then, the homogeneous equilibrium model describing the one-dimensional flow under consideration is given by

$$\left\{\begin{array}{l} \partial_t\rho + \partial_x(\rho u) = 0, \\ \partial_t(\rho u) + \partial_x(\rho u^2 + p) = 0, \\ \partial_t(\rho E) + \partial_x(\rho E + p)u = 0. \end{array}\right. \tag{16}$$

This corresponds to $\mathbf{u}^{\mathrm{E}} = (\rho, \rho u, \rho E)$, $\mathbf{f}^{\mathrm{E}}(\mathbf{u}^{\mathrm{E}}) = (\rho u, \rho u^2 + p, \rho E u + p u)$ and $\mathbf{S}^{\mathrm{E}}(\mathbf{u}^{\mathrm{E}}) = (0,0,0)$ with the notations introduced in (1). The first equation expresses the conservation of mass, while the second and the third respectively govern the conservation of momentum ρu and total energy ρE. Note that the two fluids share the same velocity u which is inherent in the homogeneous modelling. The pressure $p = p^{\mathrm{E}}(\rho,\varepsilon)$ is given by (15) while internal energy ε is linked to the vector $\mathbf{u}^{\mathrm{E}}$ by

$$\rho E = \rho\varepsilon + \frac{1}{2}\rho u^2. \tag{17}$$

Defining the following natural phase space for HEM:

$$\Omega^{\mathrm{E}} = \{\mathbf{u}^{\mathrm{E}} := (\rho, \rho u, \rho E) \in \mathbb{R}^3 / \rho > 0, \varepsilon = C_v T > 0\},$$

we are in position to state:

Lemma 2.2 *The first order convective system HEM is strictly hyperbolic over Ω^{E}, with the following eigenvalues:*

$$\lambda_1(\mathbf{u}^{\mathrm{E}}) = u - c^{\mathrm{E}} < \lambda_2(\mathbf{u}^{\mathrm{E}}) = u < \lambda_3(\mathbf{u}^{\mathrm{E}}) = u + c^{\mathrm{E}},$$

where the sound speed c^{E} is such that

$$\left(c^{\mathrm{E}}(\mathbf{u}^{\mathrm{E}})\right)^2 = \begin{cases} \gamma_1(\gamma_1-1)\varepsilon & \text{if} \quad 0 < \rho \leq \rho_1^\star, \\ (\gamma_1-1)^2\dfrac{\rho_1^{\star 2}}{\rho^2}\varepsilon = (\gamma_2-1)^2\dfrac{\rho_2^{\star 2}}{\rho^2}\varepsilon & \text{if} \quad \rho_1^\star < \rho < \rho_2^\star, \\ \gamma_2(\gamma_2-1)\varepsilon & \text{if} \quad \rho \geq \rho_2^\star. \end{cases} \tag{18}$$

Moreover, the second field is linearly degenerate.

The proof of this lemma follows from standard calculations and is left to the reader. See also [30], [13], [15], [16], [17].

Remark 3 It is worth noting that the sound speed $\mathbf{u}^{\mathrm{E}} \to c^{\mathrm{E}}(\mathbf{u}^{\mathrm{E}})$ is discontinuous when the density ρ is equal to $\rho_1^\star$ or $\rho_2^\star$. As a result, the first and the third fields, corresponding respectively to the eigenvalues $u-c^{\mathrm{E}}$ and $u+c^{\mathrm{E}}$, are neither genuinely nonlinear nor linearly degenerate. This property is known to make more complicated the resolution of the Riemann problem since admissible nonclassical solutions violating the standard selection criterion naturally arise. Such considerations are of course out of the scope of this paper. Besides, existence and uniqueness may be recovered when imposing the validity of the Liu criterion for instance. We refer for instance the reader to [30], [31] and the references therein.

Let us now address the homogeneous relaxation model.

2.2.2 The homogeneous relaxation model HRM

The homogeneous relaxation model considers that the two-phase flow no longer evolves instantaneously at thermodynamic equilibrium, but only at mechanical equilibrium. Modelling assumptions (9) are replaced by

$$p_1(\rho_1, \varepsilon_1) = p_2(\rho_2, \varepsilon_2), \tag{19}$$

that is, in the case under study,

$$(\gamma_1 - 1)\rho_1 = (\gamma_2 - 1)\rho_2 \tag{20}$$

due to (5) and (7). In other words, and contrary to HEM, densities ρ_1 and ρ_2 are not restricted any longer to take the saturation values $\rho_1^\star$ and $\rho_2^\star$, but are simply linked by the algebraic relation (20). Actually, HRM accounts for mass transfers between the two fluids assuming that the thermodynamic equilibrium $g_1(\rho_1, \varepsilon_1) = g_2(\rho_2, \varepsilon_2)$ is not instantaneously achieved, but it is reached at speed $\lambda_0 > 0$. More precisely, the system reads

$$\begin{cases} \partial_t(\rho_1 z) + \partial_x(\rho_1 z u) = \lambda_0\big(\rho_1^\star z^\star(\rho) - \rho_1 z\big), \\ \partial_t \rho + \partial_x(\rho u) = 0, \\ \partial_t(\rho u) + \partial_x(\rho u^2 + p) = 0, \\ \partial_t(\rho E) + \partial_x(\rho E + p)u = 0, \end{cases} \tag{21}$$

that is, with the notations introduced in (1), $\mathbf{u}^{\mathrm{R}} = (\rho_1 z, \rho, \rho u, \rho E)$, $\mathbf{f}^{\mathrm{R}}(\mathbf{u}^{\mathrm{R}}) = (\rho_1 z u, \rho u, \rho u^2 + p, \rho E u + p u)$ and $\mathbf{S}^{\mathrm{R}}(\mathbf{u}^{\mathrm{R}}) = (\lambda_0\big(\rho_1^\star z^\star(\rho) - \rho_1 z\big), 0, 0, 0)$. In order to close system (21), let us recall that $\rho = \rho_1 z + \rho_2(1-z)$, therefore

$$z = \frac{\rho - \rho_2}{\rho_1 - \rho_2},$$

while $z^\star(\rho)$ corresponds to the thermodynamic equilibrium value given by $\rho = \rho_1^\star z^\star(\rho) + \rho_2^\star(1 - z^\star(\rho))$ when $\rho \in [\rho_1^\star, \rho_2^\star]$. Otherwise, we naturally set $\rho_1^\star z^\star(\rho) = \rho$ if $\rho \leq \rho_1^\star$ and $\rho_1^\star z^\star(\rho) = 0$ if $\rho \geq \rho_2^\star$, so that

$$z^\star(\rho) = \begin{cases} \dfrac{\rho}{\rho_1^\star} & \text{if} \quad 0 < \rho \leq \rho_1^\star, \\ \dfrac{\rho - \rho_2^\star}{\rho_1^\star - \rho_2^\star} & \text{if} \quad \rho_1^\star \leq \rho \leq \rho_2^\star, \\ 0 & \text{if} \quad \rho \geq \rho_2^\star. \end{cases} \tag{22}$$

Note that $\rho_2 > \rho_1$ since we have assumed $\gamma_1 > \gamma_2$. Pressure p simply follows from identity $p = z p_1(\rho_1, \varepsilon) + (1-z) p_2(\rho_2, \varepsilon)$, that is

$$p = p(\rho_1 z, \rho, \varepsilon) = \big((\gamma_1 - 1)\rho_1 z + (\gamma_2 - 1)(\rho - \rho_1 z)\big)\varepsilon, \tag{23}$$

and (17) remains valid. Hereafter, this pressure law will be noted $p^{\mathrm{R}}(\rho_1 z, \rho, \varepsilon)$.

Remark 4 We note that in the limit $\lambda_0 \to +\infty$, usually called equilibrium*, HRM converges at least formally toward HEM. Indeed, the first equation in (21) leads in this asymptotic regime to the relation $\rho_1 z = \rho_1^\star z^\star(\rho)$ and we get the pressure law (15) by means of (23) and (22). In other words, $p^{\mathrm{R,eq}} := p^{\mathrm{R}}\big(\rho_1^\star z^\star(\rho), \rho, \varepsilon\big)$ equals $p^{\mathrm{E}} := p^{\mathrm{E}}(\rho, \varepsilon)$.*

To conclude, a natural phase space for HRM is

$$\Omega^{\mathrm{R}} = \{\mathbf{u}^{\mathrm{R}} := (\rho_1 z, \rho, \rho u, \rho E) \in \mathbb{R}^4 / \rho > 0,\ 0 \leq \rho_1 z \leq \rho,\ \varepsilon = C_v T > 0\},$$

and the following statement holds true.

Lemma 2.3 *The first order underlying system of HRM is hyperbolic over Ω^{R}, with the following eigenvalues:*

$$\lambda_1(\mathbf{u}^{\mathrm{R}}) = u - c^{\mathrm{R}} < \lambda_2(\mathbf{u}^{\mathrm{R}}) = \lambda_3(\mathbf{u}^{\mathrm{R}}) = u < \lambda_4(\mathbf{u}^{\mathrm{R}}) = u + c^{\mathrm{R}},$$

where the sound speed c^{R} is such that

$$\Big(c^{\mathrm{R}}(\mathbf{u}^{\mathrm{R}})\Big)^2 = \frac{A(\rho_1 z, \rho)}{\rho}\big(1 + \frac{A(\rho_1 z, \rho)}{\rho}\big)\varepsilon, \quad A(\rho_1 z, \rho) = (\gamma_1 - 1)\rho_1 z + (\gamma_2 - 1)(\rho - \rho_1 z). \tag{24}$$

Moreover, the first and fourth fields are genuinely nonlinear and the second and the third ones are linearly degenerate.

Remark 5 Let $\mathbf{u}^{\mathrm{E}}$ *be a vector of* Ω^{E} *and* $\mathbf{u}^{\mathrm{R,eq}} = \left(\rho_1^\star z^\star(\rho), \mathbf{u}^{\mathrm{E}}\right)$ *the associated vector of* Ω^{R} *taken at equilibrium. Then, it can be shown by easy calculations that* $\mathbf{c}^{\mathrm{R}}(\mathbf{u}^{\mathrm{R,eq}}) \geq \mathbf{c}^{\mathrm{E}}(\mathbf{u}^{\mathrm{E}})$ *which ensures that the first (respectively last) eigenvalue of the model HRM is less or equal (respectively greater or equal) than the first (respectively last) eigenvalue of the model HEM. This property can be related to the so-called sub-characteristic condition (or Whitham condition) that guarantees the stability of the relaxation process in relaxation systems. See for instance [9], [18] and the literature on this subject.*

3 The coupling problem

The coupling problem we study is as follows. The global problem is 1D (see [28] for coupling problems in higher dimensions). The interface coupling is $\mathcal{I} = \{x = 0\}$ and separates the two open sub-domains $\mathcal{D}^{\mathrm{E}} = \mathbb{R}^{-,*}$ and $\mathcal{D}^{\mathrm{R}} = \mathbb{R}^{+,*}$. The flow is thus governed by the following set of PDE:

$$\begin{aligned} \partial_t \mathbf{u}^{\mathrm{E}} + \partial_x \mathbf{f}^{\mathrm{E}}(\mathbf{u}^{\mathrm{E}}) &= \mathbf{S}^{\mathrm{E}}(\mathbf{u}^{\mathrm{E}}), \quad \text{for } t > 0 \text{ and } x \in \mathcal{D}^{\mathrm{E}}, \\ \partial_t \mathbf{u}^{\mathrm{R}} + \partial_x \mathbf{f}^{\mathrm{R}}(\mathbf{u}^{\mathrm{R}}) &= \mathbf{S}^{\mathrm{R}}(\mathbf{u}^{\mathrm{R}}), \quad \text{for } t > 0 \text{ and } x \in \mathcal{D}^{\mathrm{R}}, \end{aligned}$$

detailed respectively in (16) and (21), complemented by the initial data

$$\begin{aligned} \mathbf{u}^{\mathrm{E}}(x,0) &= \mathbf{u}_0^{\mathrm{E}}(x), \quad \text{for } x \in \mathcal{D}^{\mathrm{E}}, \\ \mathbf{u}^{\mathrm{R}}(x,0) &= \mathbf{u}_0^{\mathrm{R}}(x), \quad \text{for } x \in \mathcal{D}^{\mathrm{R}}, \end{aligned}$$

where $\mathbf{u}_0^{\mathrm{E}} \in \Omega^{\mathrm{E}}$ and $\mathbf{u}_0^{\mathrm{R}} \in \Omega^{\mathrm{R}}$ are given.

It remains to define the behavior of the flow through $\mathcal{I}$. Since the two models are different, there is no obvious way to couple the systems HEM and HRM. However, these models are somehow compatible (see Rem. 4) and govern the evolution of the same fluid. Therefore, the coupling should be performed in such a way that the solution obeys some physical requirements. Here, we provide three numerical coupling methods, in order to ensure respectively:

- the global conservation of ρ, ρu and ρE,
- the continuity of ρ, ρu and ρE (and the conservation of ρ) through $\mathcal{I}$,
- the continuity of ρ, ρu and p (and the conservation of ρ and ρu) through $\mathcal{I}$.

(For rigorous definitions of coupling, we refer to [25, 26].) Let us emphasize that the two latter coupling must be understood in a weak sense, since we are dealing with hyperbolic systems and discontinuous solutions. Indeed, if the characteristic speeds are incompatible, the variables expected to be constant through $\mathcal{I}$ can jump. As an example, think about the transport equation $\partial_t v + a\partial_x v = 0$, with $a > 0$ for $x < 0$ and $a < 0$ for $x > 0$. In this case, the solution will be discontinuous [25].

In the following, a numerical method of coupling is proposed for each interface coupling. Afterward, the ability of each numerical coupling method to provide approximate solutions in agreement with the corresponding coupling condition (that is either the global conservation, the continuity of the conservative variable or the continuity of the primitive variable) is illustrated by numerous numerical experiments.

4 The numerical coupling

In this section, we show how to couple the two homogeneous models from a numerical point of view. We aim at presenting several strategies, depending on informations that should be transferred through the interface and/or expected properties of the solution, in terms of conservation in particular.

Let be given a constant time step Δt and a constant space step Δx and let us set $\nu = \Delta t/\Delta x$. Introducing the cell interfaces $x_j = j\Delta x$ for $j \in \mathbb{Z}$ and $t^n = n\Delta t$ for $n \in \mathbb{N}$, we classically seek at each time t^n a piecewise constant approximate solution $x \to \mathbf{u}_\nu(x, t^n)$ of the solution $\mathbf{u}$ of the coupling problem (1):

$$\mathbf{u}_\nu(x, t^n) = \mathbf{u}^n_{j+1/2} \quad \text{for all} \quad x \in C_{j+1/2} = [x_j; x_{j+1}), \;\; j \in \mathbb{Z}, \;\; n \in \mathbb{N}.$$

Note that for $j = 0$, $x_j = x_0$ coincides with the coupling interface and, for all $n \in \mathbb{N}$, $\mathbf{u}^n_{j+1/2} = (\rho, \rho u, \rho E)^n_{j+1/2}$ has three components for $j < 0$ and $\mathbf{u}^n_{j+1/2} = (\rho_1 z, \rho, \rho u, \rho E)^n_{j+1/2}$ has four components for $j \geq 0$.

In order to advance some given sequence $(\mathbf{u}^n_{j+1/2})_{j\in\mathbb{Z}}$ at time t^n to the next time level t^{n+1}, our approach proposes two steps based on a splitting strategy between the convective parts and the source terms of HEM and HRM. More precisely:

Step 1 ($t^n \to t^{n+1-}$)
In the first step, we focus on the convective part of the coupling problem. It consists in solving

$$\begin{cases} \partial_t \mathbf{u}^{\mathrm{E}} + \partial_x \mathbf{f}^{\mathrm{E}}(\mathbf{u}^{\mathrm{E}}) = 0, & x < 0, \\ \partial_t \mathbf{u}^{\mathrm{R}} + \partial_x \mathbf{f}^{\mathrm{R}}(\mathbf{u}^{\mathrm{R}}) = 0, & x > 0, \end{cases} \tag{25}$$

for $t \in (0, \Delta t]$ with initial data $\mathbf{u}_\nu(., t^n)$ and some coupling condition which we describe below. We denote $\mathbf{u}_\nu(., t^{n+1-})$ the corresponding solution at time $t = \Delta t$.

Step 2 ($t^{n+1-} \to t^{n+1}$)
Then, $\mathbf{u}_\nu(., t^{n+1-})$ naturally serves as initial data for solving the source terms:

$$\begin{cases} \partial_t \mathbf{u}^{\mathrm{E}} = \mathbf{S}^{\mathrm{E}}(\mathbf{u}^{\mathrm{E}}), & x < 0, \\ \partial_t \mathbf{u}^{\mathrm{R}} = \mathbf{S}^{\mathrm{R}}(\mathbf{u}^{\mathrm{R}}), & x > 0, \end{cases} \tag{26}$$

again for $t \in (0, \Delta t]$. This step will provide us with an updated solution $\mathbf{u}_\nu(., t^{n+1})$ and this completes the numerical procedure.

4.1 The convective part

Let us first address the first step devoted to the convective part. In this context, we assume two schemes to be given, by mean of two 2-point numerical flux functions $\mathbf{g}^{\mathrm{E}} : \mathbb{R}^3 \times \mathbb{R}^3 \mapsto \mathbb{R}^3$ and $\mathbf{g}^{\mathrm{R}} : \mathbb{R}^4 \times \mathbb{R}^4 \mapsto \mathbb{R}^4$ respectively consistent with the flux functions $\mathbf{f}^{\mathrm{E}}$ and $\mathbf{f}^{\mathrm{R}}$ in the sense of finite volume methods. The former are used to numerically solve the first-order underlying systems of HEM and HRM on each side of the interface, that is

$$\begin{aligned} \mathbf{u}^{n+1-}_{j-1/2} &= \mathbf{u}^n_{j-1/2} - \nu(\mathbf{g}^{\mathrm{E}}_j - \mathbf{g}^{\mathrm{E}}_{j-1}), \quad j \leq 0, \\ \mathbf{u}^{n+1-}_{j+1/2} &= \mathbf{u}^n_{j+1/2} - \nu(\mathbf{g}^{\mathrm{R}}_{j+1} - \mathbf{g}^{\mathrm{R}}_j), \quad j \geq 0, \end{aligned} \tag{27}$$

with for all $j \neq 0$:

$$\mathbf{g}_j^{\mathrm{E}} = \mathbf{g}^{\mathrm{E}}(\mathbf{u}_{j-1/2}^n, \mathbf{u}_{j+1/2}^n), \quad \mathbf{g}_j^{\mathrm{R}} = \mathbf{g}^{\mathrm{R}}(\mathbf{u}_{j-1/2}^n, \mathbf{u}_{j+1/2}^n).$$

We concentrate on 3-point conservative schemes without loss of generality. At the discrete level, the coupling of HEM and HRM amounts to define the quantities $\mathbf{g}_0^{\mathrm{E}}$ and $\mathbf{g}_0^{\mathrm{R}}$. In particular, observe from now on that the first step is conservative in the quantities common to both systems, namely ρ, ρu and ρE, if and only if the last three components of $\mathbf{g}_0^{\mathrm{E}}$ and $\mathbf{g}_0^{\mathrm{R}}$ are equal. We now describe three different strategies for evaluating $\mathbf{g}_0^{\mathrm{E}}$ and $\mathbf{g}_0^{\mathrm{R}}$.

4.1.1 The flux coupling

The flux coupling strategy consists in including HEM and HRM to be coupled in a global model. The very motivation is to propose a fully conservative numerical treatment. To that purpose, let us first recall that owing to Remark 4, HEM and HRM are thermodynamically consistent, that is $p^{\mathrm{R,eq}} = p^{\mathrm{E}}$. In a rather natural way, we then consider the following HRM-like relaxation system in order to include together HEM and HRM in the same formalism:

$$\left\{ \begin{array}{l} \partial_t(\rho_1 z) + \partial_x(\rho_1 z u) = \lambda(x)\big(\rho_1^\star z^\star(\rho) - \rho_1 z\big), \\ \partial_t \rho + \partial_x(\rho u) = 0, \\ \partial_t(\rho u) + \partial_x(\rho u^2 + p) = 0, \\ \partial_t(\rho E) + \partial_x(\rho E + p) u = 0, \end{array} \right. \tag{28}$$

with $(x,t) \in \mathbb{R} \times \mathbb{R}^{+,\star}$ and

$$\lambda(x) = \left\{ \begin{array}{rcl} +\infty & \text{for} & x < 0, \\ 0 & \text{for} & x > 0. \end{array} \right. \tag{29}$$

As expected, the relaxation parameter λ is considered to be $+\infty$ for HEM, that is $\rho_1 z = \rho_1^\star z^\star(\rho)$, and 0 for HRM since for the present moment we are dealing with the convective parts only. The pressure $p = p^{\mathrm{R}}(\rho_1 z, \rho, \varepsilon)$ is still given by (23). Defining $\mathbf{u}_{-1/2}^{n,\mathrm{eq}} = \big(\rho_1^\star z^\star(\rho), \rho, \rho u, \rho E\big)_{-1/2}^n$, we are thus led to set

$$\mathbf{g}_0^{\mathrm{E}} = (g_2^{\mathrm{R}}, g_3^{\mathrm{R}}, g_4^{\mathrm{R}})(\mathbf{u}_{-1/2}^{n,\mathrm{eq}}, \mathbf{u}_{1/2}^n) \quad \text{and} \quad \mathbf{g}_0^{\mathrm{R}} = \mathbf{g}^{\mathrm{R}}(\mathbf{u}_{-1/2}^{n,\mathrm{eq}}, \mathbf{u}_{1/2}^n), \tag{30}$$

where with classical notations, $\{g_i^{\mathrm{R}}\}_{i=2,3,4}$ denotes the last three components of $\mathbf{g}^{\mathrm{R}}$.

4.1.2 The intermediate state coupling

We have just seen that the flux coupling is motivated by (and achieves) a conservation property on conservative variables $\rho, \rho u, \rho E$ common to both systems HEM and HRM. Regarding the intermediate state coupling, the idea is rather to impose the continuity of some variables of physical interest through the interface.

We first propose to impose the continuity of the common variables $\rho, \rho u, \rho E$ at the interface. So, introducing the natural vectors $\mathbf{u}_{1/2}^{n,\mathrm{E}} = (\rho, \rho u, \rho E)_{1/2}^n$ and

$\mathbf{u}^{n,\mathrm{R}}_{-1/2} = \big(\rho^\star_1 z^\star(\rho), \rho, \rho u, \rho E\big)^n_{-1/2}$ for converting a vector of HRM into a vector of HEM and *vice versa*, it gives the following natural definition for $\mathbf{g}^{\mathrm{E}}_0$ and $\mathbf{g}^{\mathrm{R}}_0$:

$$\mathbf{g}^{\mathrm{E}}_0 = \mathbf{g}^{\mathrm{E}}(\mathbf{u}^n_{-1/2}, \mathbf{u}^{n,\mathrm{E}}_{1/2}) \quad \text{and} \quad \mathbf{g}^{\mathrm{R}}_0 = \mathbf{g}^{\mathrm{R}}(\mathbf{u}^{n,\mathrm{R}}_{-1/2}, \mathbf{u}^n_{1/2}). \tag{31}$$

Remark 6 We remark that $\mathbf{u}^{n,\mathrm{R}}_{-1/2} = \mathbf{u}^{n,\mathrm{eq}}_{-1/2}$ so that (30) and (31) only differ by the definition of $\mathbf{g}^{\mathrm{E}}_0$. But in the case when $\mathbf{u}^n_{1/2}$ is at equilibrium, that is $(\rho_1 z)^n_{1/2} = \rho^\star_1 z^\star(\rho^n_{1/2})$, let us recall that the pressure p obeys equivalently (15) and (23) (see Remark 4). This implies that the last three conservation laws of HRM on ρ, ρu and ρE coincide with the three ones of HEM. From a numerical point of view, it is thus expected that $(g^{\mathrm{R}}_2, g^{\mathrm{R}}_3, g^{\mathrm{R}}_4)(\mathbf{u}^{n,\mathrm{eq}}_{-1/2}, \mathbf{u}^n_{1/2})$ and $\mathbf{g}^{\mathrm{E}}(\mathbf{u}^n_{-1/2}, \mathbf{u}^{n,\mathrm{E}}_{1/2})$ are equal, or at least very close depending on the choice of $\mathbf{g}^{\mathrm{E}}$ and $\mathbf{g}^{\mathrm{R}}$.

Definition (31) aims at providing, whenever possible, the continuity of ρ, ρu and ρE at the interface. If such a property actually holds, the internal energy ε is continuous as well by (17) but not the pressure p since generally speaking $\mathbf{u}^n_{1/2}$ is not at equilibrium, that is $\rho_1 z \neq \rho^\star_1 z^\star(\rho)$ and therefore $p^{\mathrm{E}}(\rho, \varepsilon) \neq p^{\mathrm{R}}(\rho_1 z, \rho, \varepsilon)$. That is the reason why we now propose to modify the initial intermediate state coupling in order to impose the continuity of the pressure p and let us say ρ and ρu. The latter choice is natural to achieve conservation of mass ρ and momentum ρu. We then define two vectors, $\overline{\mathbf{u}}^{n,\mathrm{E}}_{1/2}$ for HEM and $\overline{\mathbf{u}}^{n,\mathrm{R}}_{-1/2}$ for HRM, sharing the same ρ, ρu and p as $\mathbf{u}^n_{1/2}$ and $\mathbf{u}^n_{-1/2}$ respectively:

$$\overline{\mathbf{u}}^{n,\mathrm{E}}_{1/2} = (\rho, \rho u, \overline{\rho E}^{\mathrm{E}})^n_{1/2} \quad \text{and} \quad \overline{\mathbf{u}}^{n,\mathrm{R}}_{-1/2} = \big(\rho^\star_1 z^\star(\rho), \rho, \rho u, \overline{\rho E}^{\mathrm{R}}\big)^n_{-1/2}.$$

This is done by inverting the pressure laws (15) and (23) with respect to ε. Using in addition (17), straightforward calculations give:

$$\overline{\rho E}^{\mathrm{E}} = \frac{1}{2}\frac{(\rho u)^2}{\rho} + \begin{cases} \dfrac{p}{(\gamma_1 - 1)} & \text{if} \quad \rho \leq \rho^\star_1, \\ \dfrac{p}{(\gamma_1 - 1)}\dfrac{\rho}{\rho^\star_1} & \text{if} \quad \rho^\star_1 < \rho < \rho^\star_2, \\ \dfrac{p}{(\gamma_2 - 1)} & \text{if} \quad \rho \geq \rho^\star_2 \end{cases}$$

and

$$\overline{\rho E}^{\mathrm{R}} = \frac{1}{2}\frac{(\rho u)^2}{\rho} + \frac{\rho p}{(\gamma_1 - 1)\rho^\star_1 z^\star(\rho) + (\gamma_2 - 1)\big(\rho - \rho^\star_1 z^\star(\rho)\big)}.$$

Then we set:

$$\mathbf{g}^{\mathrm{E}}_0 = \mathbf{g}^{\mathrm{E}}(\mathbf{u}^n_{-1/2}, \overline{\mathbf{u}}^{n,\mathrm{E}}_{1/2}) \quad \text{and} \quad \mathbf{g}^{\mathrm{R}}_0 = \mathbf{g}^{\mathrm{R}}(\overline{\mathbf{u}}^{n,\mathrm{R}}_{-1/2}, \mathbf{u}^n_{1/2}). \tag{32}$$

Remark 7 The state $\overline{\mathbf{u}}^{n,\mathrm{R}}_{-1/2}$ being at equilibrium, it is clear that $\overline{\rho E}^{\mathrm{R}\,n}_{-1/2}$ equals $\rho E^n_{-1/2}$. As an immediate consequence we have $\overline{\mathbf{u}}^{n,\mathrm{R}}_{-1/2} = \mathbf{u}^{n,\mathrm{R}}_{-1/2}$ and both flux coupling and intermediate state coupling strategies (modified or not) only differ by $\mathbf{g}^E_0$ (see also Remark 6).

Remark 8 Let us also note that if $\mathbf{u}_{1/2}^n$ *is at equilibrium, the corresponding pressure* $p_{1/2}^n$ *may well be computed using either* p^{E} *or* p^{R} *so that* $\overline{\mathbf{u}}_{1/2}^{n,\mathrm{E}} = \mathbf{u}_{1/2}^{n,\mathrm{E}}$ *and both intermediate state coupling strategies (modified or not) have the same* $\mathbf{g}_0^{\mathrm{E}}$*. Hence and by Remark 6, the three coupling strategies are expected to be equal in this (very particular) situation.*

To conclude this section, let us keep in mind that in general $\mathbf{g}_0^{\mathrm{E}} \neq \mathbf{g}_0^{\mathrm{R}}$ for the intermediate state coupling strategy (modified or not). Therefore, the first step of the whole numerical procedure is not conservative in ρ, ρu and ρE contrary to the flux coupling strategy.

4.2 The source term

This section is devoted to the numerical treatment of (26). Since $\mathbf{S}^{\mathrm{E}} = (0,0,0)$ and $\mathbf{S}^{\mathrm{R}} = (\lambda_0(\rho_1^\star z^\star(\rho) - \rho_1 z), 0, 0, 0)$, we naturally set

$$\left\{ \begin{array}{l} \rho_{j+1/2}^{n+1} = \rho_{j+1/2}^{n+1-}, \\ u_{j+1/2}^{n+1} = u_{j+1/2}^{n+1-}, \\ E_{j+1/2}^{n+1} = E_{j+1/2}^{n+1-}, \end{array} \right. \qquad \forall j \in \mathbb{Z}, n \in \mathbb{N}$$

since ρ, ρu and ρe do not vary in this step. It remains to solve

$$\partial_t \rho_1 z = \lambda_0(\rho_1^\star z^\star(\rho) - \rho_1 z)$$

in each cell of $\mathcal{D}^{\mathrm{R}}$. This is done exactly via the formula

$${\rho_1}_{j+1/2}^{n+1} z_{j+1/2}^{n+1} = \rho_1^\star z^\star(\rho_{j+1/2}^{n+1-}) - \left(\rho_1^\star z^\star(\rho_{j+1/2}^{n+1-}) - {\rho_1}_{j+1/2}^{n+1-} z_{j+1/2}^{n+1-}\right) e^{-\lambda_0 \Delta t},$$

for all $j \in \mathbb{N}$ and $n \in \mathbb{N}$.

4.3 The numerical schemes

We present now the numerical schemes we have tested, that is, we give several possible definitions for $\mathbf{g}^{\mathrm{E}}$ and $\mathbf{g}^{\mathrm{R}}$. The first scheme is the Rusanov scheme [34], which is a very simple, but diffusive, scheme. The second scheme is a standard Lagrange-Projection scheme, as proposed in [20]. In opposition to the previous one, this method is an upwinding scheme, but not a 3-point scheme (it is actually a 5-point scheme and the numerical flux also depends on $\nu = \Delta t/\Delta x$). The third scheme is a nonconservative modification of the Lagrange-Projection scheme first introduced in [4, 8], in order to avoid spurious oscillations of pressure near contact discontinuities.

4.3.1 The Rusanov scheme

The Rusanov scheme [34] is a classical 3-point scheme. The associated numerical flux is

$$\mathbf{g}^\alpha(\mathbf{u},\mathbf{v}) = \frac{\mathbf{f}^\alpha(\mathbf{u}) + \mathbf{f}^\alpha(\mathbf{v})}{2} - \frac{\lambda_m^\alpha(\mathbf{u},\mathbf{v})}{2}(\mathbf{v}-\mathbf{u}), \tag{33}$$

with

$$\lambda_m^\alpha(\mathbf{u},\mathbf{v}) = \max(\max_i(|\lambda_i^\alpha(\mathbf{u})|), \max_i(|\lambda_i^\alpha(\mathbf{v})|))$$

where λ_i^α is the i-th eigenvalue of the jacobian matrix $\mathrm{D}\mathbf{f}^\alpha$, $\alpha = E, R$. Under the classical CFL condition

$$\nu \max_j(\max_i |\lambda_i^\alpha(\mathbf{u}_{j+1/2}^n)|) \leq C < \frac{1}{2},$$

the Rusanov scheme is positive for the density and stable (C is called the Courant number). This scheme is very simple but it is very diffusive, which is due to the central, but stable, discretization (opposed to an upwind discretization). When considering for instance stationary contact discontinuities (null velocity, uniform pressure and non uniform density), the Rusanov scheme cannot preserve such profiles, the density is diffused, contrarily to usual upwind schemes like Godunov method or Lagrange-Projection schemes. We will see the consequences of this drawback in the numerical results.

4.3.2 The Lagrange-Projection scheme

Lagrange-Projection schemes are based on an operator splitting consisting in solving first the Euler equations in pseudo-Lagrangian coordinates ($t^n \to t^{n+1/2}$) and then the advection part of the equations ($t^{n+1/2} \to t^{n+1-}$), which may appear as a projection procedure on the fixed mesh. The exact Godunov scheme associated with this splitting is described in [24]. We prefer here to use an approximate Godunov resolution of the Lagrange part. This Lagrangian scheme can be interpreted as an acoustic scheme (see [21]) or a relaxation scheme (see [19]). The Lagrange step of the scheme for HRM is

$$\left\{\begin{array}{l} {\rho_1}_{j+1/2}^{n+1/2} z_{j+1/2}^{n+1/2} = \rho_{j+1/2}^{n+1/2} \dfrac{{\rho_1}_{j+1/2}^n z_{j+1/2}^n}{\rho_{j+1/2}^n}, \\ \rho_{j+1/2}^{n+1/2} = \dfrac{\rho_{j+1/2}^n}{1+\nu\left(u_{j+1}^n - u_j^n\right)}, \\ u_{j+1/2}^{n+1/2} = u_{j+1/2}^n - \dfrac{\nu}{\rho_{j+1/2}^n}\left(p_{j+1}^n - p_j^n\right), \\ E_{j+1/2}^{n+1/2} = E_{j+1/2}^n - \dfrac{\nu}{\rho_{j+1/2}^n}\left(p_{j+1}^n u_{j+1}^n - p_j^n u_j^n\right) \end{array}\right.$$

with

$$\left\{\begin{array}{l} u_j^n = \frac{1}{2(\rho c)_j^n}(p_{j-1/2}^n - p_{j+1/2}^n) + \frac{1}{2}(u_{j-1/2}^n + u_{j+1/2}^n), \\ p_j^n = \frac{1}{2}(p_{j-1/2}^n + p_{j+1/2}^n) + \frac{(\rho c)_j^n}{2}(u_{j-1/2}^n - u_{j+1/2}^n), \end{array}\right.$$

the approximate local Lagrangian sound speed $(\rho c)_j^n$ above being given by

$$(\rho c)_j^n = \sqrt{\max(\rho_{j-1/2}^n {c_{j-1/2}^n}^2, \rho_{j+1/2}^n {c_{j+1/2}^n}^2)\min(\rho_{j-1/2}^n, \rho_{j+1/2}^n)}$$

where $c_{j+1/2}^n$ is the sound speed in cell $j+1/2$ at time step n: $c_{j+1/2}^n = c^{\mathbf{R}}(\mathbf{u}_{j+1/2}^n)$. Quantities $p_{j+1/2}^n$ are to be understood in the same sense,

$$p_{j+1/2}^n = p^{\mathbf{R}}\left({\rho_1}_{j+1/2}^n z_{j+1/2}^n, \rho_{j+1/2}^n, E_{j+1/2}^n - 1/2\left(u_{j+1/2}^n\right)^2\right)$$

for all j under consideration.

Then, the projection step enables to compute

$$\left(\rho_1{}_{j+1/2}^{n+1-} z_{j+1/2}^{n+1-}, \rho_{j+1/2}^{n+1-}, \rho_{j+1/2}^{n+1-} u_{j+1/2}^{n+1-}, \rho_{j+1/2}^{n+1-} E_{j+1/2}^{n+1-}\right).$$

The whole Lagrange-Projection time step for HRM results in the following flux:

$$\mathbf{g}_j^{\mathrm{R}} = \begin{pmatrix} \widetilde{\rho_1}_j^n \tilde{z}_j^n u_j^n \\ \tilde{\rho}_j^n u_j^n \\ \tilde{\rho}_j^n \tilde{u}_j^n u_j^n + p_j^n \\ \tilde{\rho}_j^n \tilde{E}_j^n u_j^n + p_j^n u_j^n \end{pmatrix}$$

(see above for the fluxes u_j^n and p_j^n) with

$$\text{if } u_j^n \geq 0, \begin{cases} \widetilde{\rho_1}_j^n \tilde{z}_j^n = \rho_1{}_{j-1/2}^{n+1/2} z_{j-1/2}^{n+1/2}, \\ \tilde{\rho}_j^n = \rho_{j-1/2}^{n+1/2}, \\ \tilde{u}_j^n = u_{j-1/2}^{n+1/2}, \\ \tilde{E}_j^n = E_{j-1/2}^{n+1/2}, \end{cases} \quad \text{and if } u_j^n < 0, \begin{cases} \widetilde{\rho_1}_j^n \tilde{z}_j^n = \rho_1{}_{j+1/2}^{n+1/2} z_{j+1}^{n+1/2}, \\ \tilde{\rho}_j^n = \rho_{j+1/2}^{n+1/2}, \\ \tilde{u}_j^n = u_{j+1/2}^{n+1/2}, \\ \tilde{E}_j^n = E_{j+1/2}^{n+1/2}. \end{cases}$$

The flux $\mathbf{g}_j^{\mathrm{E}}$ for HEM follows the same definition and is composed of the last three components of $\mathbf{g}_j^{\mathrm{R}}$.

Note that because of the definition of $\widetilde{\rho_1}_j^n \tilde{z}_j^n$, $\tilde{\rho}_j^n$, $\tilde{u}_j^n$ and $\tilde{E}_j^n$, this is a 4-point flux. This leads to define four vectors instead of two for the numerical coupling: $\overline{\mathbf{u}}_{-3/2}^{n,\mathrm{R}}$ and $\overline{\mathbf{u}}_{-1/2}^{n,\mathrm{R}}$ for HRM, and $\overline{\mathbf{u}}_{1/2}^{n,\mathrm{E}}$ and $\overline{\mathbf{u}}_{3/2}^{n,\mathrm{E}}$ for HEM.

This scheme has the drawback of creating spurious oscillations near contact discontinuities when dealing with a non-ideal gas such as in HEM and HRM. For this reason we propose a slight modification of the Lagrange-Projection scheme to avoid this phenomenon. The modification is based on the fact that the oscillations come up in the projection procedure, the Lagrange step being oscillation-free whatever the pressure law. Thus we propose to project the quantities $\rho_1 z$, ρ, ρu, and p instead of ρE,which implies a maximum principle on p in the projection step. This new scheme is oscillation-free near contact discontinuities but has the drawback of being nonconservative in total energy. Nevertheless in the following numerical test-cases where shocks are not too strong, we do not observe important artefacts. This scheme will be called "nonconservative Lagrange-Projection scheme" and noted L-PP in the following. Let us briefly give the scheme for HRM. The only difference concerns the quantity ρE. It is updated in two steps. In the Lagrange step, the same formulas as above are used, and we compute $p_{j+1/2}^{n+1/2} = \left(\rho_1{}_{j+1/2}^{n+1/2} z_{j+1/2}^{n+1/2}, \rho_{j+1/2}^{n+1/2}, E_{j+1/2}^{n+1/2} - 1/2\left(u_{j+1/2}^{n+1/2}\right)^2\right)$. Then, the unknowns $(\rho_1 z, \rho, \rho u)$ are updated in the same way as with the conservative Lagrange-Projection scheme, but not E. We here compute first $p_{j+1/2}^{n+1-}$ as

$$p_{j+1/2}^{n+1-} = p_{j+1/2}^{n+1/2} - \nu\left(u_{j+1}^n(\tilde{p}_{j+1}^n - p_{j+1/2}^{n+1/2}) - u_j^n(\tilde{p}_j^n - p_{j+1/2}^{n+1/2})\right)$$

with

$$\text{if } u_j^n \geq 0, \quad \tilde{p}_j^n = p_{j-1/2}^{n+1/2}, \quad \text{and if } u_j^n < 0, \quad \tilde{p}_j^n = p_{j+1/2}^{n+1/2}.$$

Finally, we compute $E_{j+1/2}^{n+1-}$ by inverting the pressure law, finding $E_{j+1/2}^{n+1-}$ such that

$$p^{\mathbf{R}}\left(\rho_1{}_{j+1/2}^{n+1-} z_{j+1/2}^{n+1-}, \rho_{j+1/2}^{n+1-}, E_{j+1/2}^{n+1-} - 1/2\left(u_{j+1/2}^{n+1-}\right)^2\right) = p_{j+1/2}^{n+1-}.$$

The nonconservative scheme for HEM is a straightforward transposition of this one.

5 Numerical experiments

In this section, several numerical tests are presented in order to illustrate the different behaviors obtained at the coupling interface, according to the numerical scheme and the numerical coupling we use. In all the experiments, the computational space domain is $[-1/2; 1/2]$, the associated mesh is composed of 500 cells and the Courant number C equals 0.4. We will always consider Riemann initial data given by

$$\begin{array}{l} \mathbf{u}^{\mathrm{E}}(0,x) = \mathbf{u}_l, \quad -1/2 \leq x < 0, \\ \mathbf{u}^{\mathrm{R}}(0,x) = \mathbf{u}_r, \quad 0 < x \leq 1/2, \end{array} \tag{34}$$

where $\mathbf{u}_l \in \Omega^{\mathrm{E}}$ and $\mathbf{u}_r \in \Omega^{\mathrm{R}}$ are two constant states. Actually, the initial data will be given with respect to the variable $\mathbf{v} = (\rho, u, p)$. More precisely, $\mathbf{u}_l = (\rho_l, \rho_l u_l, \rho(\varepsilon^{\mathrm{E}}(\rho_l, p_l) + (u_l)^2/2))$ where $\varepsilon^{\mathrm{E}}(\rho, p)$ is given by inverting (15) and $\mathbf{u}_r = ((\rho_1)_r z_r, \rho_r, \rho_r u_r, \rho(\varepsilon^{\mathrm{R}}((\rho_1)_r z_r, \rho_r, p_r) + (u_r)^2/2))$ where

$$(\rho_1)_r = \frac{\rho_r}{z_r + \frac{\gamma_1 - 1}{\gamma_2 - 1}(1 - z_r)}, \tag{35}$$

and $\varepsilon^{\mathrm{R}}(\rho_1 z, \rho, p)$ is provided by (23). Besides, the initial data for the HRM part will be given with respect to the variable $(c, \mathbf{v})$, where c is the mass fraction of vapor and is plotted in each figure. It is defined by $c = \rho_1^\star z^\star(\rho)/\rho$ for $x < 0$ and by $c = \rho_1 z/\rho$ for $x > 0$, and it naturally lies between 0 and 1.

The specific heat C_v is equal to 1, and the values of the adiabatic coefficients are $\gamma_1 = 1.6$ and $\gamma_2 = 1.4$, which leads to $\rho_1^\star \approx 0.613132$ and $\rho_2^\star \approx 0.919699$, using (13) (below, these values will be plotted on each graph of the density variable).

The first five tests illustrate the ability of the different coupling methods to provide the continuity at the coupling interface of $(\rho u, \rho u^2 + p, u(\rho E + p))$ for the flux coupling, of $(\rho, \rho u, \rho E)$ for the intermediate state coupling with the conservative variable and of (ρ, u, p) for the modified intermediate state coupling. In order to make the results we present as clear as possible, the source term of HRM is not taken into account in these five experiments. In the sixth one, the numerical convergence of the coupling model between HEM and HRM toward a global HEM, letting λ_0 increase, is investigated.

5.1 A simple test in phase 2

We begin these numerical tests with a very simple case. The data of this test are

	c	ρ	u	p
$\mathbf{v}_l$	$-$	2	0	1
$(c,\mathbf{v})_r$	0	1.5	0	2

$t_m = 0.2, \quad \lambda_0 = 0,$ (36)

where t_m represents the time at which the solutions are plotted. One may remark that the HRM part of the domain is initially at equilibrium ($z_r = z^\star(\rho_r)$), so that HRM becomes equivalent to HEM. Moreover, let us emphasize that this solution is totally involved in phase 2 (that is $\rho > \rho_2^\star$). Therefore, the global solution of the coupling problem corresponds to the one provided by a unique system HEM, defined everywhere in the domain of computation. Due to these particular properties of the initial data, the three numerical coupling methods must give the same results (see also Rem. 6 and 8), which may be seen in Figs. 1, 2 and 3. One may also check that the Rusanov scheme is more diffusive than the Lagrange-Projection schemes.

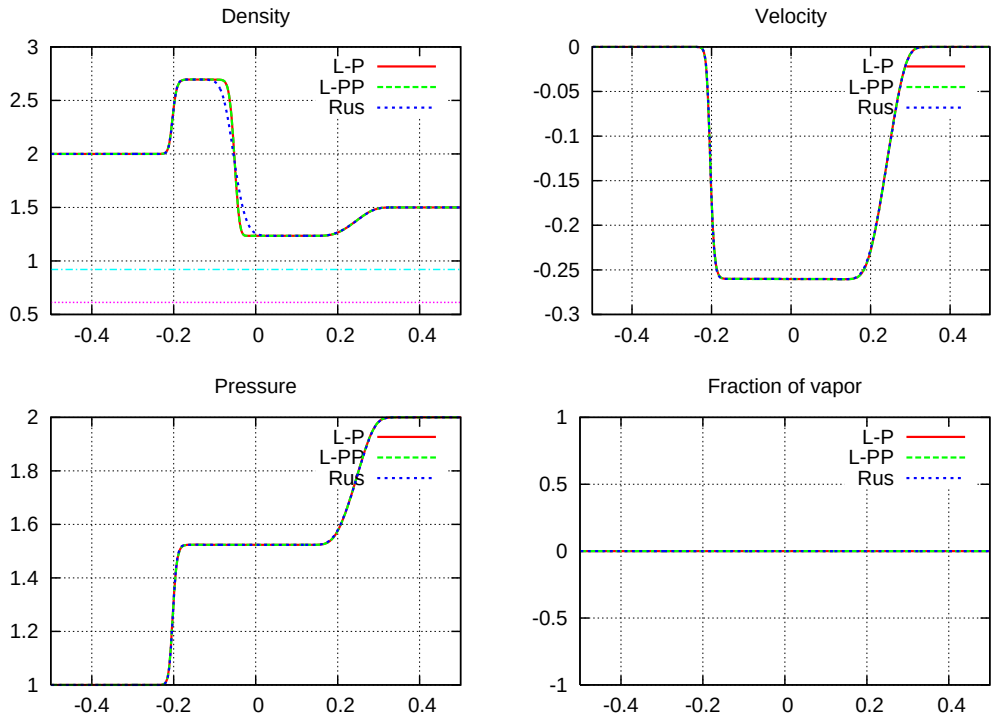

Figure 1: A test in phase 2 (36): Intermediate state coupling (conservative variable). Lagrange-Projection (L-P), nonconservative Lagrange-Projection (L-PP) and Rusanov scheme (Rus).

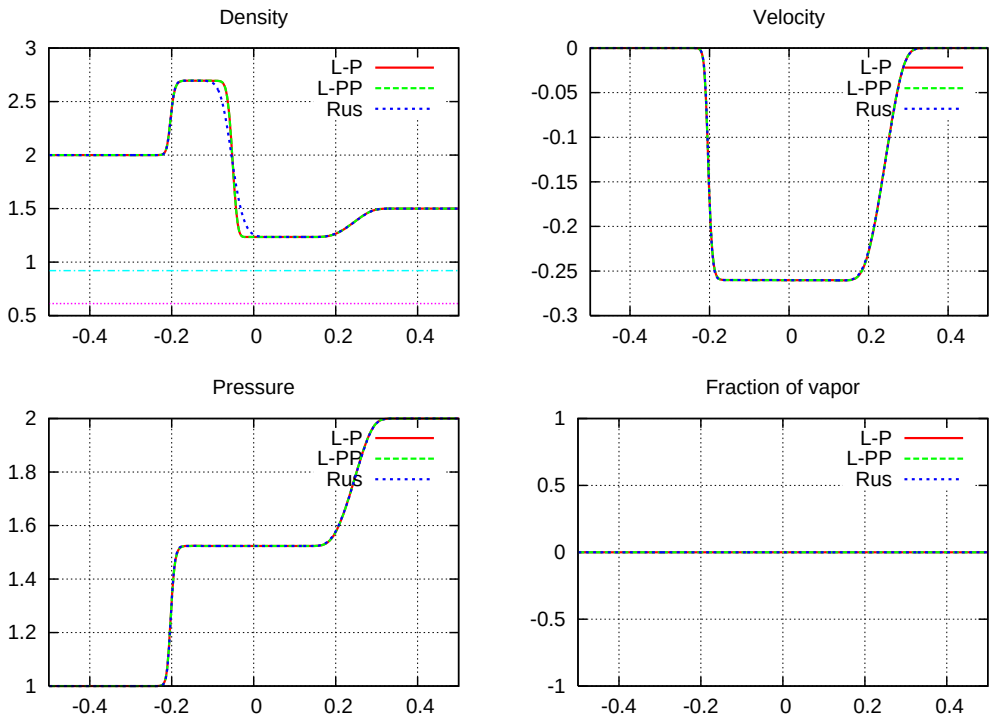

Figure 2: A test in phase 2 (36): Intermediate state coupling (nonconservative variable). Lagrange-Projection (L-P), nonconservative Lagrange-Projection (L-PP) and Rusanov scheme (Rus).

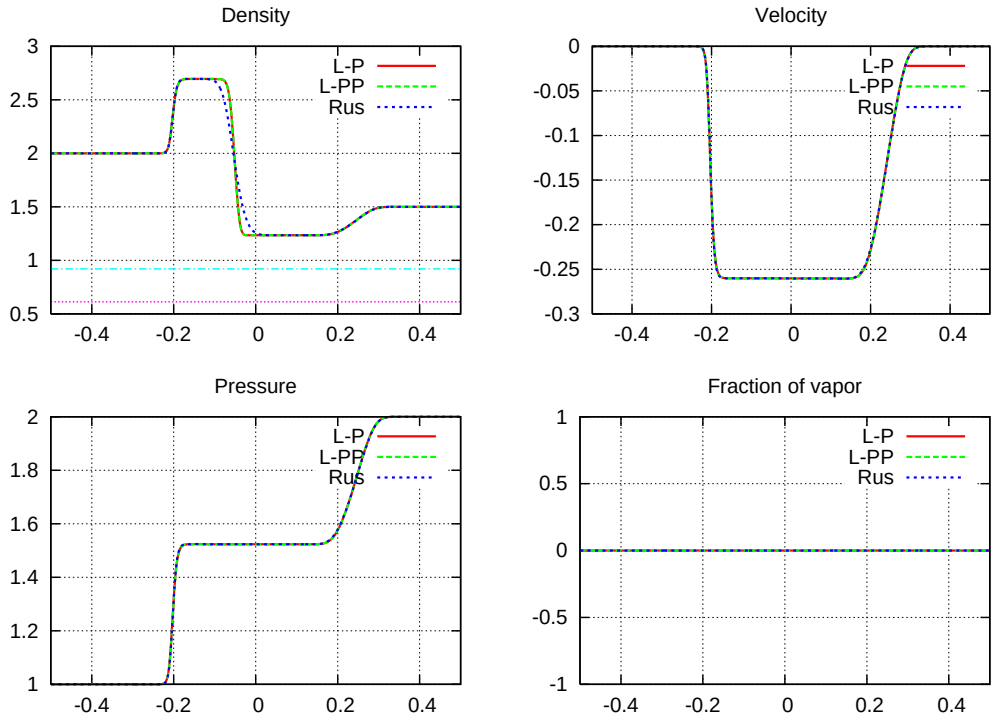

Figure 3: A test in phase 2 (36): Flux coupling. Lagrange-Projection (L-P), non-conservative Lagrange-Projection (L-PP) and Rusanov scheme (Rus).

5.2 Uniform velocity and pressure at equilibrium

In this case, the right part of the domain is still at equilibrium, but the left part and the right part belong to different phases since $\rho_l > \rho_2^\star$ and $\rho_r < \rho_1^\star$. Since $z_r = z^\star(\rho_r)$, this test enters in the frame described in Rem. 6 and 8. The numerical results of the different coupling methods are thus expected to be very close. The data associated with this test are

	c	ρ	u	p
$\mathbf{v}_l$	$-$	2	1	1
$(c,\mathbf{v})_r$	1	0.5	1	1

$t_m = 0.15, \quad \lambda_0 = 0,$ (37)

so that the solution is composed by a contact discontinuity, moving to the right, that is in the HRM part of the domain. Since the contact discontinuity separates the two phases, the adiabatic coefficients are different on both sides of the wave and it is well-known that, in such case, any standard conservative scheme provides spurious oscillations on the profiles of u and p (see for instance [1]). Basically, only

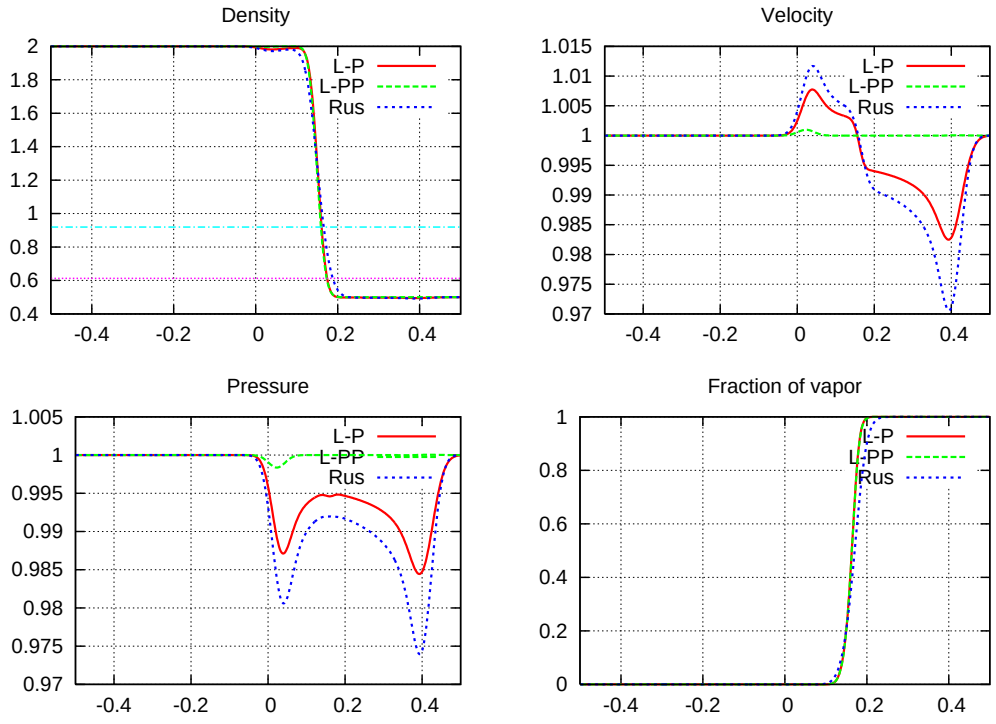

Figure 4: Uniform velocity and pressure at equilibrium (37): Intermediate state coupling (conservative variable). Lagrange-Projection (L-P), nonconservative Lagrange-Projection (L-PP) and Rusanov scheme (Rus).

the nonconservative Lagrange-Projection scheme can maintain the velocity and the pressure constant, that is exactly the reason why this scheme has been introduced (see also [4, 8]). Nevertheless, as mentioned above, the intermediate state coupling

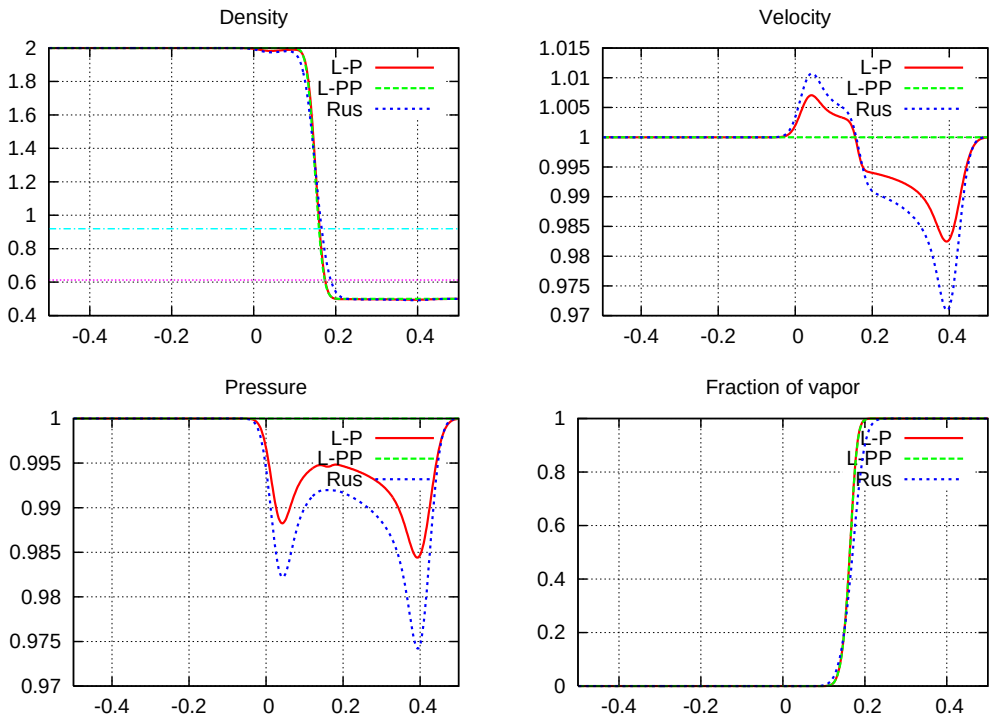

Figure 5: Uniform velocity and pressure at equilibrium (37): Intermediate state coupling (nonconservative variable). Lagrange-Projection (L-P), nonconservative Lagrange-Projection (L-PP) and Rusanov scheme (Rus).

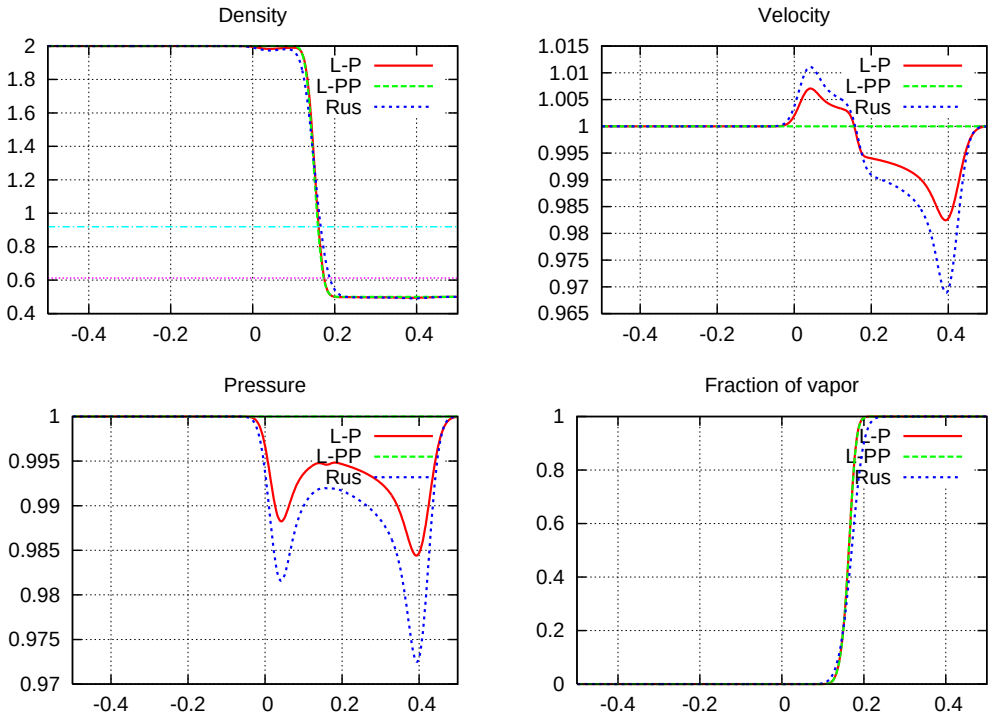

Figure 6: Uniform velocity and pressure at equilibrium (37): Flux coupling. Lagrange-Projection (L-P), nonconservative Lagrange-Projection (L-PP) and Rusanov scheme (Rus).

with the conservative variable modifies the pressure through the coupling interface. Consequently, variations of pressure and velocity can be observed in Fig. 4 even for the nonconservative Lagrange-Projection scheme L-PP.

5.3 Uniform conservative variables out of equilibrium

We now focus on initial data out of equilibrium, that is $z_r \neq z^\star(\rho_r)$. The initial data of this test case is

	c	ρ	u	p
$\mathbf{v}_l$	$-$	2	1	1
$(c, \mathbf{v})_r$	1	2	1	1.5

$t_m = 0.15, \quad \lambda_0 = 0.$ (38)

One may check by a simple calculation that $(\rho_l, (\rho u)_l, (\rho E)_l) = (\rho_r, (\rho u)_r, (\rho E)_r)$ and $z_\star(\rho_l) \neq z_r$. In both models, the evolution in time of the conservative variables

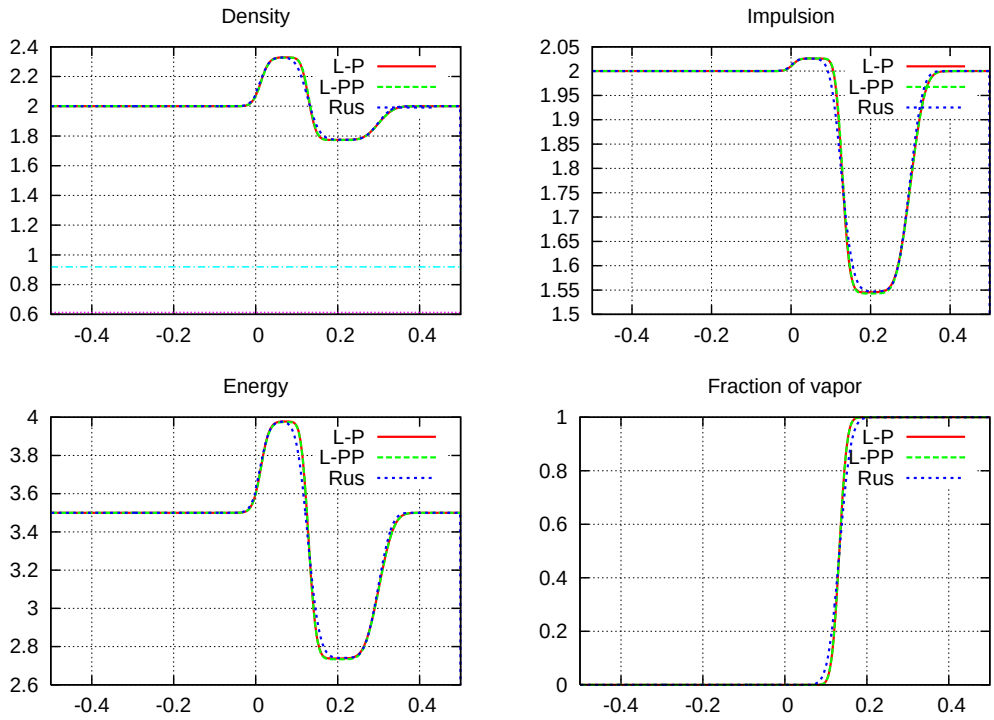

Figure 7: Uniform conservative variables out of equilibrium (38): Intermediate state coupling (conservative variable). Lagrange-Projection (L-P), nonconservative Lagrange-Projection (L-PP) and Rusanov scheme (Rus).

ρ, ρu and ρE is partially due to the spatial variation of the pressure $\partial_x p$. Here, the pressure is initially discontinuous at the coupling interface (because $z^\star(\rho_l) \neq z_r$) and thus ρ, ρu and ρE cannot remain constant for $t > 0$, even when using the intermediate state coupling with the conservative variable, see Fig. 7. Besides, since the velocity is positive, the discontinuity moves to the right and after some time

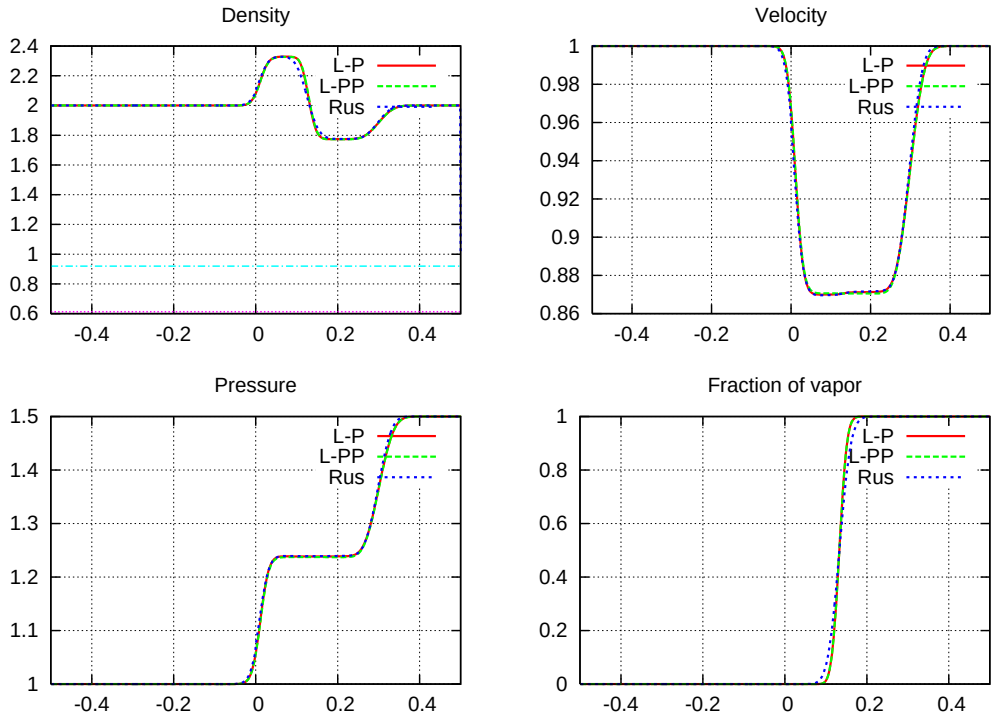

Figure 8: Uniform conservative variables out of equilibrium (38): Intermediate state coupling (nonconservative variable). Lagrange-Projection (L-P), nonconservative Lagrange-Projection (L-PP) and Rusanov scheme (Rus).

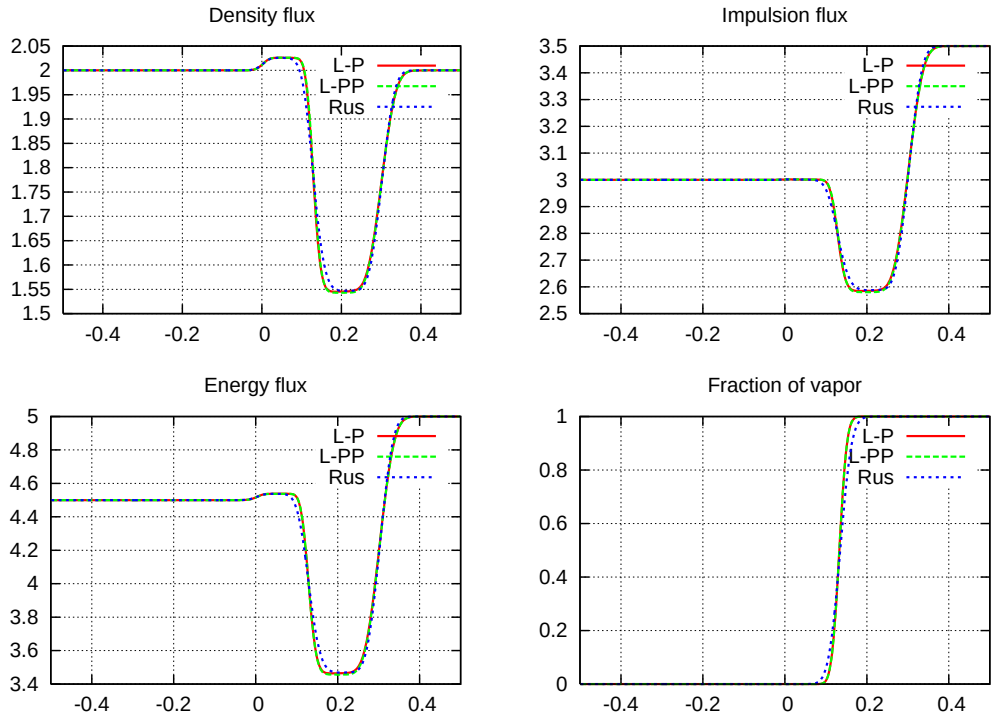

Figure 9: Uniform conservative variables out of equilibrium (38): Flux coupling. Lagrange-Projection (L-P), nonconservative Lagrange-Projection (L-PP) and Rusanov scheme (Rus).

steps, the cell $[x_0, x_1]$ is at equilibrium (i.e. $z^n_{1/2} = z^\star(\rho^n_{1/2})$), leading to a continuous pressure law through the coupling interface $x = 0$. As a result, all the variables are continuous through this interface (see Figs. 7, 8 and 9, where we have plotted the variable corresponding to the coupling method we used).

5.4 Uniform primitive variables out of equilibrium

In this case, the HRM part is still out of equilibrium:

	c	ρ	u	p
$\mathbf{v}_l$	$-$	1	-0.5	1
$(c, \mathbf{v})_r$	1	1	-0.5	1

$t_m = 0.2, \quad \lambda_0 = 0.$ (39)

Let us note that the density, the velocity and the pressure (that are the primitive variables) are the same on both sides of the coupling interface. In fact, if the state $(c, \mathbf{v})_r$ was at equilibrium, the primitive variables would be preserved constant by all the numerical methods, as we saw in the results of Section 5.2. But, for this test, the equation of state changes at the coupling interface (since $z_r \neq z^\star(\rho_r)$) and solutions with complex structures can be developed.

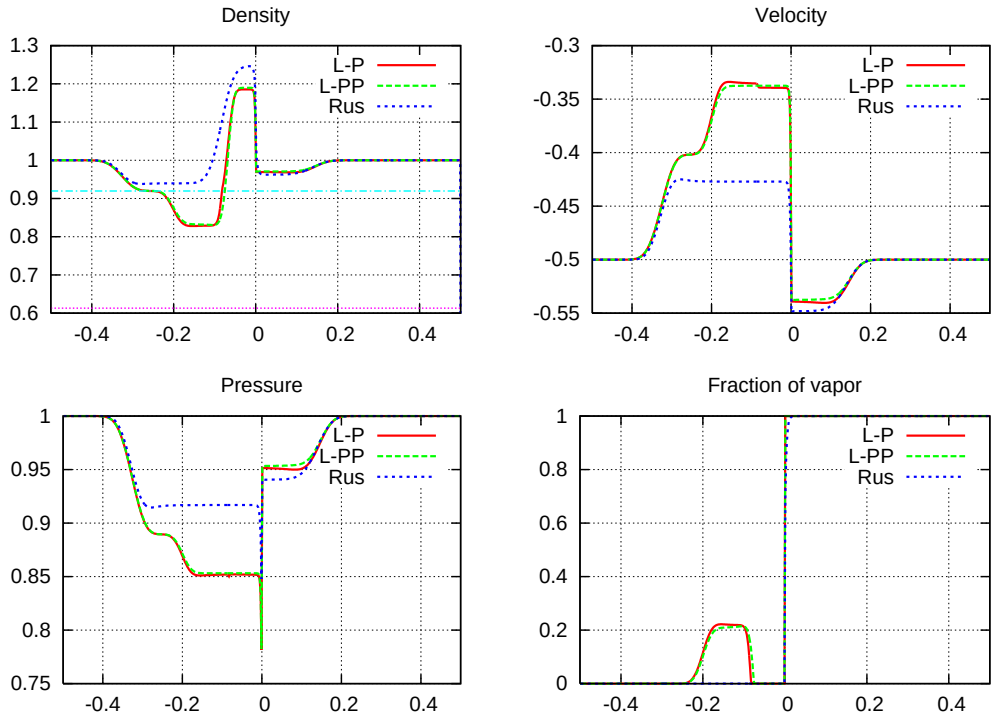

Figure 10: Uniform velocity and pressure out of equilibrium (39): Intermediate state coupling (conservative variable). Lagrange-Projection (L-P), nonconservative Lagrange-Projection (L-PP) and Rusanov scheme (Rus).

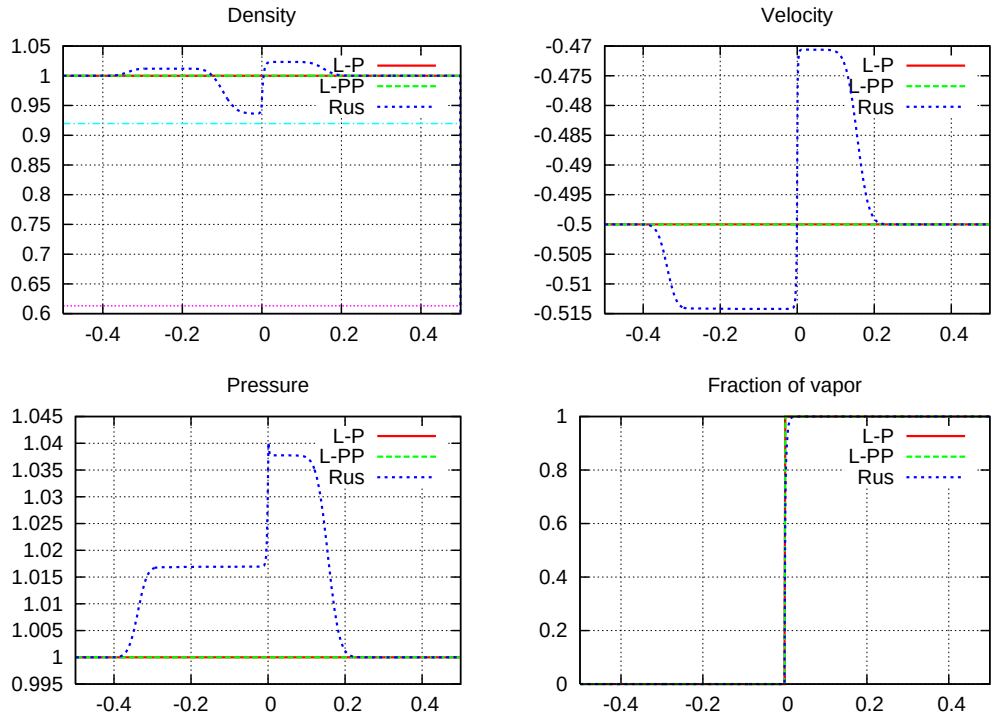

Figure 11: Uniform velocity and pressure out of equilibrium (39): Intermediate state coupling (nonconservative variable). Lagrange-Projection (L-P), nonconservative Lagrange-Projection (L-PP) and Rusanov scheme (Rus).

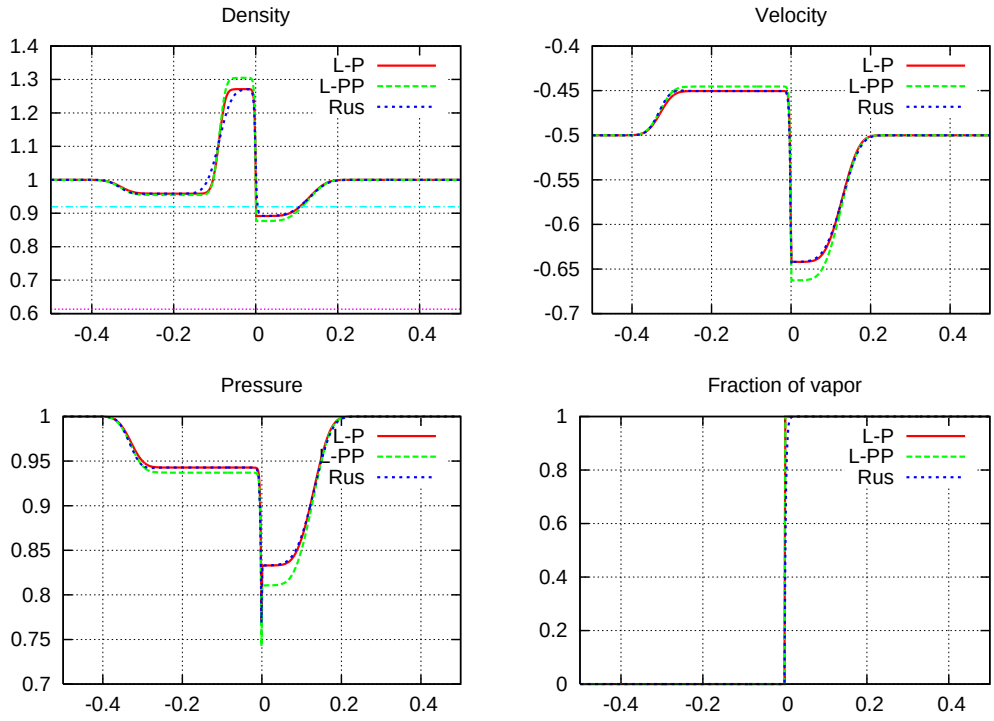

Figure 12: Uniform velocity and pressure out of equilibrium (39): Flux coupling. Lagrange-Projection (L-P), nonconservative Lagrange-Projection (L-PP) and Rusanov scheme (Rus).

Only the two Lagrange-Projection schemes with the intermediate state coupling based on the nonconservative variable $(\rho, \rho u, p)$ preserve the primitive variables constant (see Fig. 11), all other methods introduce acoustic waves in the solution (Figs. 10, 11 and 12), notice the mixture zone in Fig. 10). More precisely, since the equation of state is different on both sides of the coupling interface, the flux coupling and the intermediate state coupling based on the conservative variable provide different values of the pressure from the one side to the other side and thus, introduce acoustic waves.

The reason why the Rusanov scheme with the modified intermediate state coupling introduces acoustic waves is different. As we mentioned, the Rusanov scheme is very diffusive. Therefore, the coupling interface is slightly "diffused" by the Rusanov scheme, in the sense that, in the first cell at the right of the coupling interface, c no longer exactly equals either 0 or 1 but lies strictly in $(0, 1)$ (see the shape of the fraction of vapor in Fig. 11). The direct consequence is a modification of the pressure in the cell at the right of the coupling interface and thus, the pressure cannot be left constant.

5.5 Shock tube with occurrence of phase 1

In this test, the initial condition is at equilibrium:

	c	ρ	u	p
$\mathbf{v}_l$	$-$	1	-2	1
$(c, \mathbf{v})_r$	0	1	1	1
$t_m = 0.1, \quad \lambda_0 = 0,$				

(40)

but, whereas the initial condition is in phase 2, an intermediate zone with $\rho < \rho_1^\star$ appears for $t > 0$, overlapping the coupling interface. Therefore, $c = 1$ in the HEM part of the intermediate zone but since the velocity at $x = 0$ is negative, the fraction c stays equal to 0 in the HRM part of the intermediate zone. As in the previous case, the discontinuity of z leads to a discontinuity of the pressure law. Therefore, only the coupling method based on the nonconservative variable provides a continuous pressure through $x = 0$, see Fig. 14. In Fig. 15 are plotted the results obtained by the flux coupling. The variables ρu, $\rho u^2 + p$ and $u(\rho E + p)$ are represented and one may see that, as expected, they are constant through the coupling interface. However, in Fig. 13, the variables ρ, ρu and ρE are discontinuous at $x = 0$, though these results correspond to the intermediate state coupling with the conservative variable. Indeed, we have seen in Sec. 5.3 (see also Fig. 7) that if the HRM part is out of equilibrium, the continuity of the conservative variables cannot be achieved (in test of Sec. 5.3, this leads to the appearance of acoustic waves). In the present case, since c, and thus z, is discontinuous at $x = 0$ (for all $t > 0$), the conservative variables are discontinuous at the coupling interface.

5.6 Convergence of HRM towards equilibrium

This test is based on a uniform velocity and a uniform pressure. Moreover, the HRM part is out of equilibrium (this test is similar to the test of Sec. 5.4, except for the

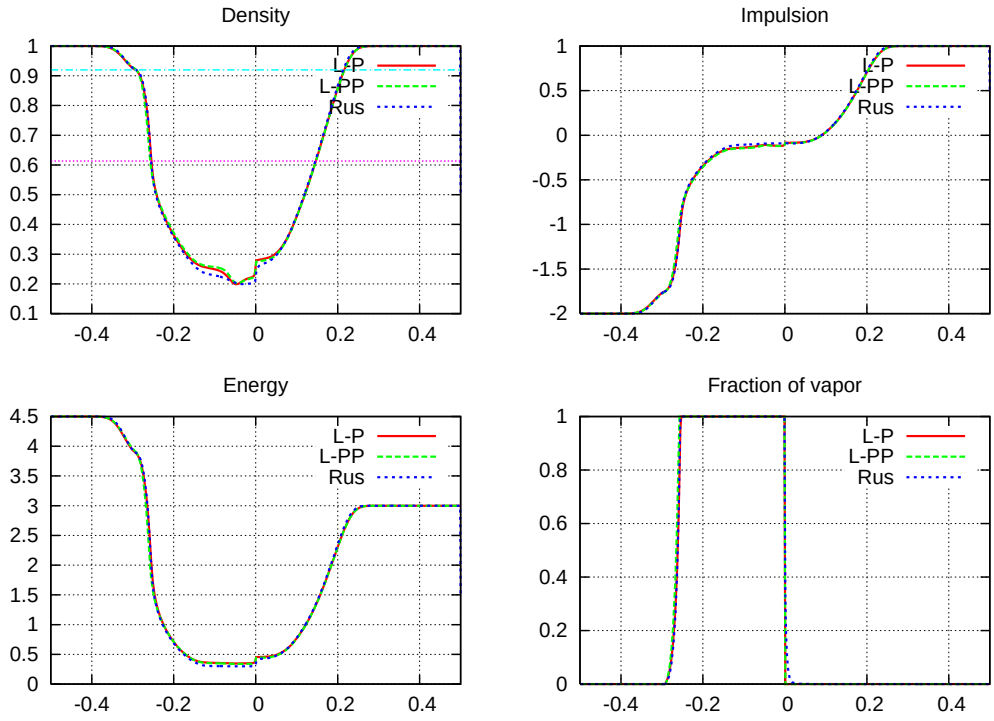

Figure 13: Shock tube with occurrence of phase 1 (40): Intermediate state coupling (conservative variable). Lagrange-Projection (L-P), nonconservative Lagrange-Projection (L-PP) and Rusanov scheme (Rus).

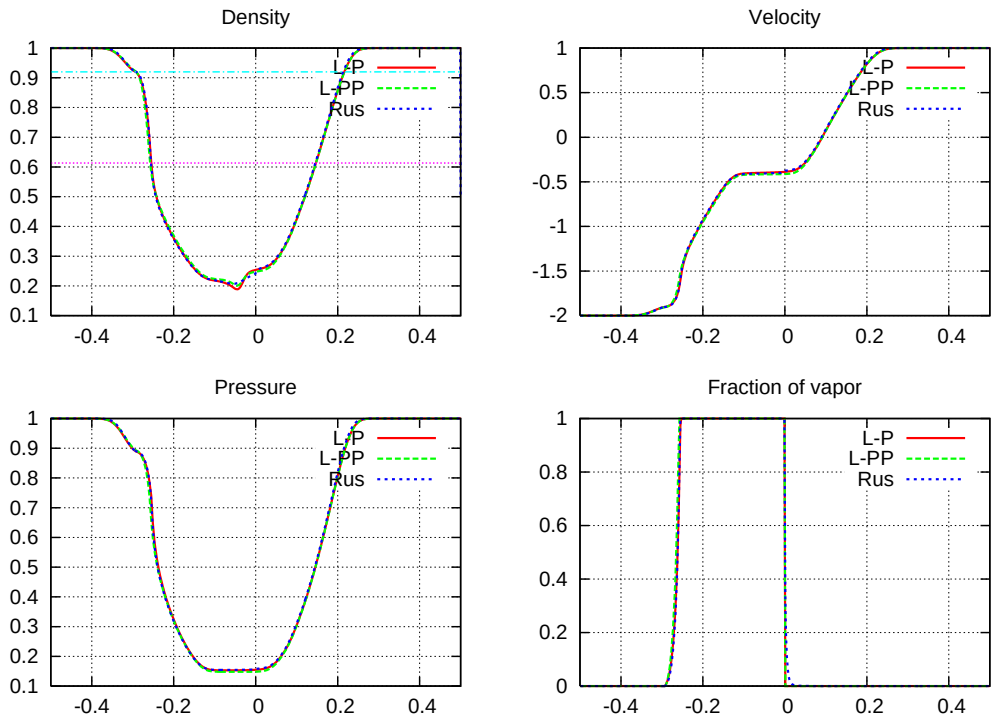

Figure 14: Shock tube with occurrence of phase 1 (40): Intermediate state coupling (nonconservative variable). Lagrange-Projection (L-P), nonconservative Lagrange-Projection (L-PP) and Rusanov scheme (Rus).

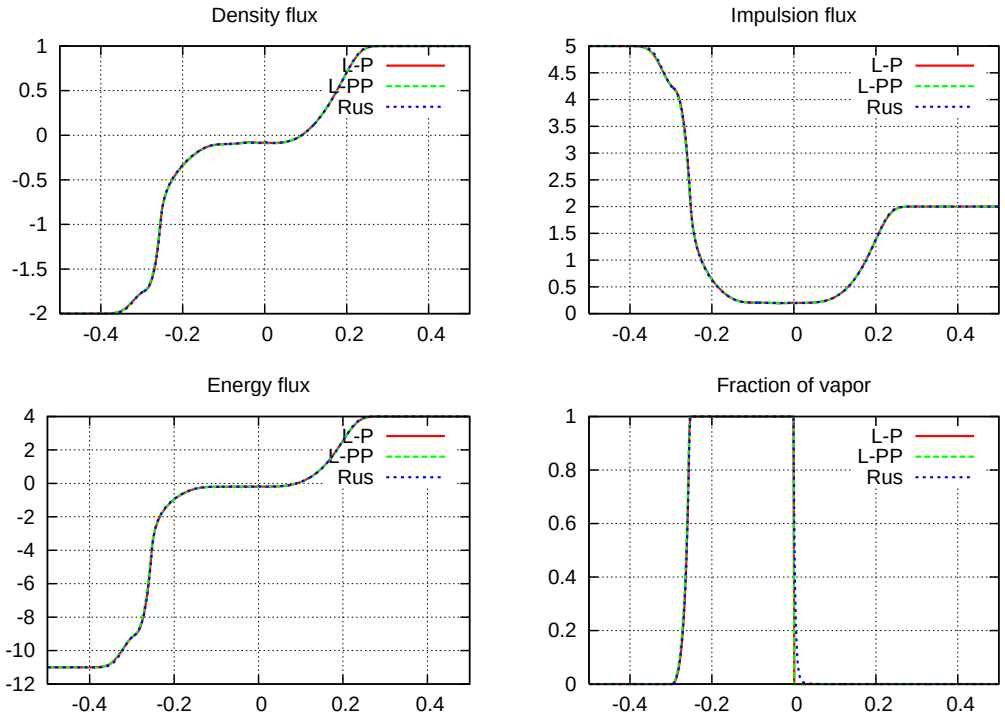

Figure 15: Shock tube with occurrence of phase 1 (40): Flux coupling. Lagrange-Projection (L-P), nonconservative Lagrange-Projection (L-PP) and Rusanov scheme (Rus).

density). We use different values of the relaxation parameter λ_0 in HRM:

	c	ρ	u	p
$\mathbf{v}_l$	$-$	1	-0.5	1
$(c,\mathbf{v})_r$	1	2	-0.5	1

$t_m = 0.2, \quad \lambda_0 = 0, 10, 100.$ (41)

As we mentioned in Rem. 4, HRM formally tends to HEM when $\lambda_0 \to +\infty$. This is the result we want to test, adding the difficulty of the numerical coupling at $x = 0$. But, before commenting the numerical results, let us study the solution expected for large λ_0. One may think naively that the limit solution would be the HEM solution associated with the initial data

	ρ	u	p
$\mathbf{v}_l$	1	-0.5	1
$\mathbf{v}_r$	2	-0.5	1

(42)

But, for the coupling problem, z_r tends to $z^\star(\rho_r)$. As a consequence, the pressure is modified in the HRM part since p^R depends on $\rho_1 z$ and, as noted before, $(\rho_1 z)_r \neq \rho_1^\star z^\star(\rho_r)$. On the contrary, the pressure of the solution of HEM with data (42) remains constant (in time and space). Then, what is the limit solution? In fact, it is the HEM solution with the initial data

	ρ	u	p
$\mathbf{v}_l$	1	-0.5	1
$\tilde{\mathbf{v}}_r$	2	-0.5	$2/3$

(43)

since, using Rem. 4 and (35), we have

$$\begin{aligned}\tilde{p}_r &= p^{\mathrm{R,eq}}(\rho_r, \varepsilon^{\mathrm{R}}((\rho_1)_r z^\star(\rho_r), \rho_r, p_r)),\\ &= p^{\mathrm{R,eq}}(2, \varepsilon^{\mathrm{R}}(0, 2, 1)),\\ &= 2/3.\end{aligned}$$

In Figs. 16, 17 and 18 are plotted the results for several λ_0, using the Lagrange-Projection scheme. One may see that, as expected, all the coupling methods tends to the solution based on HEM with data (43), whatever the numerical scheme and the coupling method.

6 Conclusion

We have shown that the coupling problem (1) can be numerically solved, once it is completed with an *interface model* that restores the continuity of physics. It must be noted that there is a multiple choice of interface models that can apply, depending on the physics that is under study. Moreover, in each case, we are able to give a numerical treatment that will verify the constraints imposed by the interfacial model, at least in a weak sense. The application of the interface coupling developed

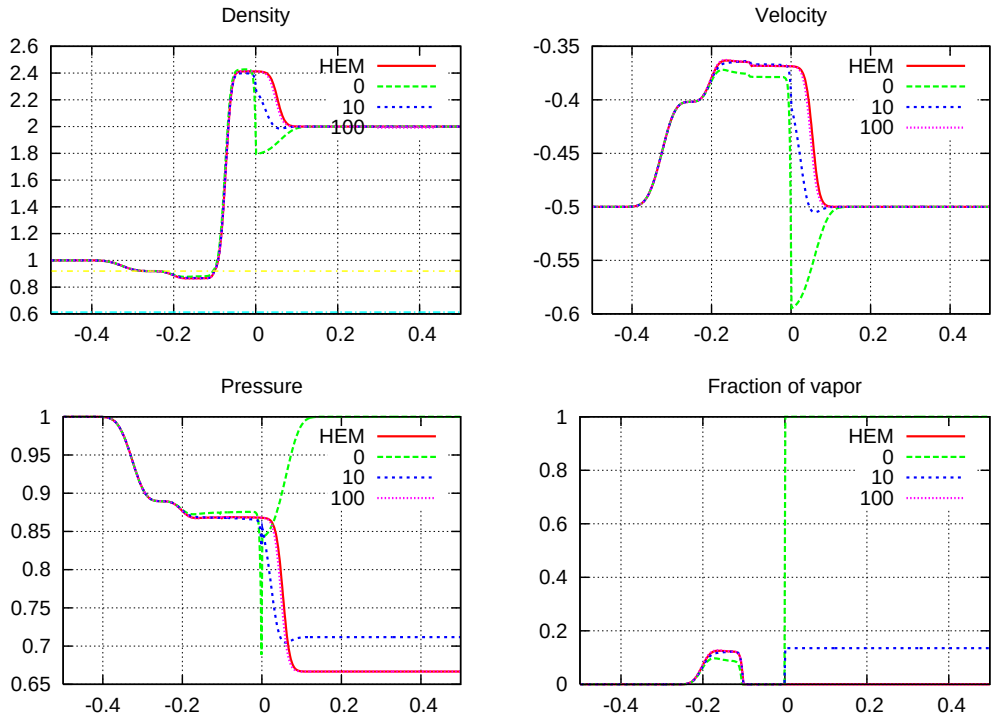

Figure 16: Convergence towards equilibrium (41): Intermediate state coupling (conservative variable). Lagrange-Projection scheme for different λ_0.

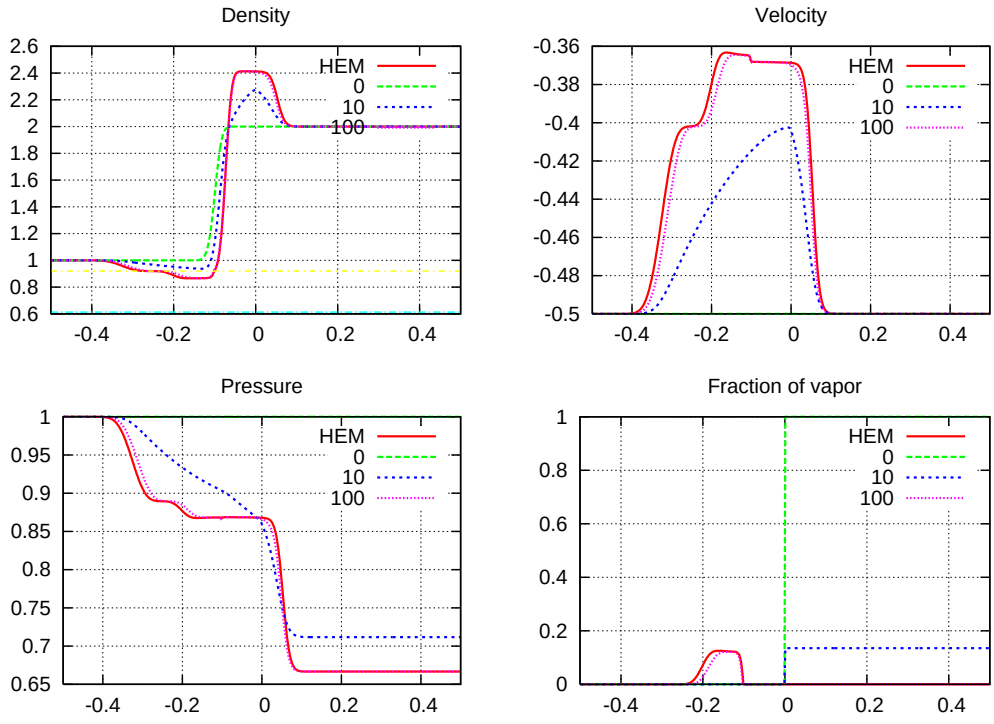

Figure 17: Convergence towards equilibrium (41): Intermediate state coupling (non-conservative variable). Lagrange-Projection scheme for different λ_0.

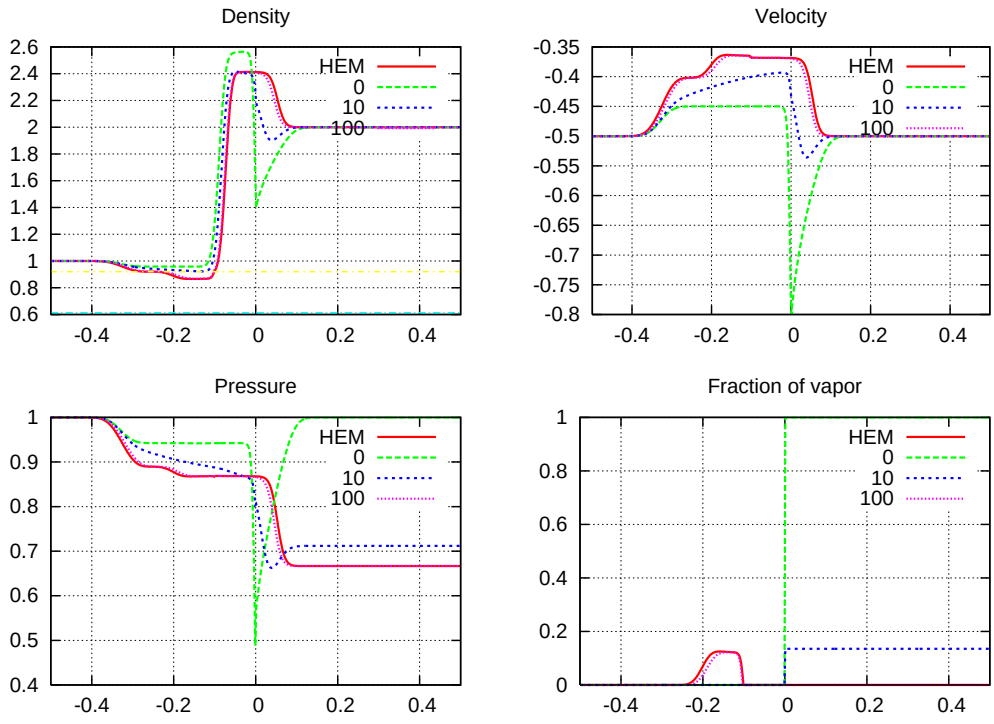

Figure 18: Convergence towards equilibrium (41): Flux coupling. Lagrange-Projection scheme for different λ_0.

here to other types of numerical methods is not the aim of this paper but seems *a priori* possible.

At last, let us mention that the numerical coupling techniques presented here are being developed in other contexts: gas dynamics (cf. [4], [5]) and Lagrangian models of gas dynamics (in [7]) and that the theory of the interface coupling is under study, based on the pioneering works [25] and [26]. In particular, the analysis of solutions to Riemann problems for the coupling of systems of gas dynamics is developed in [14] and the coupling of HEM and HRM models is analyzed from a theoretical point of view in [12].

Acknowledgements

This work was partially supported by the NEPTUNE project, funded by CEA, EDF, IRSN and AREVA-NP.

References

[1] R. Abgrall. How to prevent pressure oscillations in multicomponent flow calculations: a quasi-conservative approach. *J. Comput. Phys.*, 125(1):150–160, 1996.

[2] R. Abgrall, S. Karni. Computation of compressible multifluids. *J. Comput. Phys.*, 169:594–623, 2001.

[3] G. Allaire, G. Faccanoni, S. Kokh. *A Strictly Hyperbolic Equilibrium Phase Transition Model*, submitted.

[4] A. Ambroso, Ch. Chalons, F. Coquel, E. Godlewski, J.-M. Hérard, F. Lagoutière, P.-A. Raviart, N. Seguin. The coupling of multiphase flow models. *Proceedings of Nureth-11*, Avignon, France, 2005.

[5] A. Ambroso, Ch. Chalons, F. Coquel, E. Godlewski, F. Lagoutière, P.-A. Raviart, N. Seguin. Couplage de deux systèmes de la dynamique des gaz. *Proceedings of Congrès Français de Mécanique*, Troyes, France, 2005.

[6] A. Ambroso, Ch. Chalons, F. Coquel, E. Godlewski, F. Lagoutière, P.-A. Raviart, N. Seguin. Homogeneous models with phase transition: coupling by Finite Volume methods. *Proceedings of Finite volumes for complex applications IV (Marrakech, 2005)*, Hermes Science plubisher, 483–392, 2005.

[7] A. Ambroso, Ch. Chalons, F. Coquel, E. Godlewski, F. Lagoutière, P.-A. Raviart, N. Seguin. Extension of interface coupling to general Lagrangian systems. *Proceedings of ENUMATH*, Santiago de Compostela, Spain, 2005.

[8] T. Barberon, P. Helluy, S. Rouy. Practical computation of axisymmetrical multifluid flows. *Int. J. Finite Volumes*, 1–34, 2003.

[9] F. Bouchut. Nonlinear stability of finite volume methods for hyperbolic conservation laws, and well-balanced schemes for source. Frontiers in Mathematics Series, Birkhauser, 2004.

[10] Z. Bilicki, J. Kestin. Physical aspects of the relaxation model in two-phase flow. *Proc. R. Soc. Lond.*, A428(1875):379–397, 1990.

[11] B. Boutin. Couplage de systèmes de lois de conservation scalaires par une régularisation de Dafermos. *Master dissertation*, Paris, 2005.

[12] F. Caetano. *Sur certains problèmes de linéarisation et de couplage pour les systèmes hyperboliques non linéaires.* PhD Thesis, Université Pierre et Marie Curie-Paris6, 2006.

[13] F. Caro. *Modélisation et simulation numérique des transitions de phase liquide vapeur.* PhD thesis, CMAP, École Polytechnique, 2004.

[14] Ch. Chalons, P.-A. Raviart and N. Seguin. *The interface coupling of the gas dynamics equations.* In preparation.

[15] F. Caro, F. Coquel, D. Jamet, and S. Kokh. DINMOD: A diffuse interface model for two-phase flows modelling. In S. Cordier, T. Goudon, M. Gutnic, and E. Sonnendrücker, editors, *Numerical methods for hyperbolic and kinetic problems, IRMA lecture in mathematics and theoretical physics (Proceedings of the CEMRACS 2003)*, 2005.

[16] F. Caro, F. Coquel, D. Jamet, and S. Kokh. Phase change simulation for isothermal compressible two-phase flows. In *AIAA Comp. Fluid Dynamics*, number AIAA-2005-4697, 2005.

[17] F. Caro, F. Coquel, D. Jamet, and S. Kokh. *A Simple Finite-Volume Method for Compressible Isothermal Two-Phase Flows Simulation.* Int. J. of Finite Vol. Meth., 2006.

[18] Ch. Chalons, F. Coquel. Navier-Stokes equations with several independent pressure laws and explicit predictor-corrector schemes. *Numer. Math.*, 101(3):451-478, 2005.

[19] F. Coquel, E. Godlewski, B. Perthame, A. In, M. Rascle. Some new Godunov and relaxation methods for two-phase flow problems. Godunov methods (Oxford, 1999), 179–188, Kluwer/Plenum, New York, 2001.

[20] B. Després. Symétrisation en variable de Lagrange pour la mécanique des milieux continus et schémas numériques. *Matapli*, 72:45–61, 2003.

[21] B. Després. Invariance properties of Lagrangian systems of conservation laws, approximate Riemann solvers and the entropy condition. *Numer. Math.*, 89(1):99–134, 2001.

[22] P. Downar-Zapolski, Z. Bilicki, L. Bolle and J. Franco. The non equilibrium model for one-dimensionnal flashing liquid flow. *Int. J. Multiphase Flow*, 22(3):473–483, 1996.

[23] G. Faccanoni. *Modélisation fine d'écoulements diphasiques : contribution à l'étude de la crise d'ébullition.* Ph.D. Thesis, École Polytechnique, in preparation.

[24] E. Godlewski and P.-A. Raviart. Numerical approximation of hyperbolic systems of conservation laws. Applied Mathematical Sciences, 118. Springer-Verlag, New York, 1996.

[25] E. Godlewski and P.-A. Raviart. The numerical interface coupling of nonlinear hyperbolic systems of conservation laws. I. The scalar case. *Numer. Math.*, 97(1):81–130, 2004.

[26] E. Godlewski, K.-C. Le Thanh and P.-A. Raviart. The numerical interface coupling of nonlinear hyperbolic systems of conservation laws: II. The case of systems. *RAIRO Modél. Math. Anal. Numér*, 39(4):649–692, 2005.

[27] J.-M. Hérard. Schemes to couple flows between free and porous medium. *AIAA paper 2005-4861*, 2005.

[28] J.-M. Hérard, O. Hurisse. Coupling two and one-dimensional models through a thin interface. *AIAA paper 2005-4718*, 2005.

[29] J.-M. Hérard, O. Hurisse. A method to couple two-phase flow models. *EDF Internal Report HI-81/06/001/A*, France.

[30] S. Jaouen. *Étude mathématique et numérique de stabilité pour des modèles hydrodynamiques avec transition de phase.* PhD Thesis, Université Pierre et Marie Curie-Paris6, 2001.

[31] Ph. G. LeFloch. Hyperbolic Systems of Conservation Laws: The theory of classical and nonclassical shock waves. E.T.H. Lecture Notes Series, Birkhäuser, 2002.

[32] R. P. Fedkiw, T. Aslam, B. Merriman, S. Osher. A non-oscillatory Eulerian approach to interfaces in multimaterial flows (the ghost fluid method). *J. Comput. Phys.*, 152(2):457–492, 1999.

[33] J. Piraux, B. Lombard. A new interface method for hyperbolic problems with discontinuous coefficients: one-dimensional acoustic example. *J. Comp. Phys.*, 168(1):227–248, 2001.

[34] V. V. Rusanov. The calculation of the interaction of non-stationary shock waves with barriers. *Ž. Vyčisl. Mat. i Mat. Fiz.*, 1:267–279, 1961.

[35] C. Zhang and R. J. LeVeque. The Immersed Interface Method for acoustic wave equations with discontinuous coefficients. *Wave Motion*, 25:237–263, 1997.